Electronic Supplementary Material (ESI) for Dalton Transactions.

Supporting Information for:

Synthesis and characterisation of boranediyl- and diboranediyl-bridged diplatinum A-frame complexes

Carina Brunecker,[a,b] Merle Arrowsmith,[a,b] Jonas H. Müssig,[a,b] Julian Böhnke,[a,b] Andreas Stoy,[a,b] Merlin Heß,[a,b] Alexander Hofmann,[a,b] Carsten Lenczyk,[a,b] Crispin Lichtenberg,[a] Jacqueline Ramler,[a] Anna Rempel,[a,b] and Holger Braunschweig[a,b,]*

[a] *Institute for Inorganic Chemistry, Julius-Maximilians-Universität Würzburg, Am Hubland, 97074 Würzburg (Germany).*

[b] *Institute for Sustainable Chemistry & Catalysis with Boron, Julius-Maximilians-Universität Würzburg, Am Hubland, 97074 Würzburg (Germany).*

Table of contents

Methods and materials

All manipulations were performed either under an atmosphere of dry argon or *in vacuo* using standard Schlenk line or glovebox techniques. Deuterated solvents were dried over molecular sieves and degassed by three freeze-pump-thaw cycles prior to use. All other solvents were distilled and degassed from appropriate drying agents. Solvents (both deuterated and non-deuterated) were stored under argon over activated 4 Å molecular sieves. NMR spectra were acquired on a Bruker Avance 500 NMR spectrometer (^{1}H and ^{1}H{^{31}P}: 500.1 MHz, ^{11}B{^{1}H}: 160.5 MHz, ^{13}C{^{1}H}: 125.8 MHz, ^{31}P{^{1}H}: 202.5 MHz), Bruker Avance 400 NMR spectrometer (^{1}H: 400.1 MHz, ^{11}B{^{1}H}: 128.4 MHz, ^{13}C{^{1}H}: 100.6 MHz, ^{31}P{^{1}H}: 162.0 MHz), a Av NEO 400 SB spectrometer (^{195}Pt{^{1}H}: 86.0 MHz). Chemical shifts (δ) are given in ppm and internally referenced to the carbon nuclei (^{13}C{^{1}H}) or residual protons (^{1}H) of the solvent. ^{11}B{^{1}H}, ^{31}P{^{1}H} and ^{195}Pt{^{1}H} NMR spectra were referenced to [$BF_3{\cdot}OEt_2$], 85% H_3PO_4 or $Na_2[PtCl_6]$ as an external standard. Microanalyses (C, H, N) were performed on an Elementar vario MICRO cube elemental analyser.

Solvents and reagents were were purchased from Sigma Aldrich or Alfa Aesar. Deuterated solvents were degassed with three freeze-pump-thaw cycles and stored over molecular sieves in J. Young-style ampoules or in a glovebox. [Pt(nbe)$_3$] (nbe = norbornene),[1] BCl_2Dur (Dur = 2,3,5,6-tetramethylphenyl),[2] BCl_2Tip (Tip = 2,4,6-tri*iso*propylphenyl),[3] BCl_2NPh_2,[4] BBr_2Cy (Cy = cyclohexyl),[5] BBr_2Mes (Mes = 2,4,6-trimethylphenyl),[6] $B_2Cl_2(NMe_2)_2$[7] and complex **2**[8] were synthesised using literature procedures or based on literature procedures.

Synthetic procedures

Syntheses of Pt_2 precursors

$[Pt_2(\mu\text{-dmpm})_3]$, 1

$[Pt(nbe)_3]$ (252 mg, 529 µmol) was dissolved in benzene (10 mL) and a solution of dmpm (= bis(dimethylphosphino)methane) in benzene (340 mM, 2.76 mL, 925 µmol) was added. The red reaction mixture was stirred for 1 h at ambient temperature before removal of volatiles under reduced pressure. The solid residue was extracted with hexane and the filtrate dried, the solvent was then removed under reduced pressure and **1** (406 mg, 508 mmol, 96% based on Pt) was isolated as a red solid. The compound is fluxional at rt in solution, giving rise to very broad NMR resonances. ^1H NMR (400.1 MHz, C_6D_6): δ = 1.66 (t, $^2J_{HP}$ = 14.2 Hz, 48H, CH_3), 1.39-1.76 (v. br., 6H, CH_2) ppm. $^{13}C\{^1H\}$ NMR (100.6 MHz, C_6D_6): δ = 26.8 (s, CH_3) ppm. *Note: the* CH_2 *resonance was too broad to detect via* $^{13}C\{^1H\}$ *NMR, HSQC or HMBC.* $^{31}P\{^1H\}$ NMR (162.0 MHz, C_6D_6): δ = 8.7 (br s, $^1J_{PPt}$ = 4325 Hz) ppm. Elemental analysis (%) calculated for $[C_{15}H_{42}P_6Pt_2]$ (M_W = 798.51): C 23.59, H 5.69; found: C 23.97, H 5.56.

$[\{Pt_2(\mu\text{-dmpm})_3\}_2(\mu\text{-dmpm})]$, 3

$[Pt(nbe)_3]$ (230 mg, 481 µmol) was dissolved in benzene (10 mL) and dmpm (131 mg, 963 µmol) was added at 0 °C. The red reaction mixture was stirred for 20 min at ambient temperature and all volatiles were removed under reduced pressure at 100 °C. After extraction with hexane (3 x 10 mL) the red solid was recrystallised from hexane to give **3** (165 mg, 96.5 mmol, 80% based on Pt) as a red solid. The compound is highly fluxional at rt in solution, giving rise to very broad NMR resonances. ^1H NMR (400.1 MHz, C_6D_6): δ = 2.62 (br., 12H, CH_3), 2.09 (br., 12H, CH_2), 1.70 (t, $^2J_{HP}$ = 26 Hz, 72H, CH_3), 1.48 (br., 12H, CH_2) ppm. ***Note:*** *$^{13}C\{^1H\}$ NMR data could not be acquired owing to the poor solubility of **3**.* $^{31}P\{^1H\}$ NMR (162.0 MHz, C_6D_6): δ = −20 (broad higher-order resonance, $^1J_{PPt} \approx 4500$ Hz, $_{P\text{-}Pt3}$), −54 (broad higher-order resonance, $^1J_{PPt} \approx 4000$ Hz, $P_{P\text{-}Pt3}$), −61 (broad higher-order resonance, $P_{P\text{-}Pt3}$) ppm. Elemental analysis (%) calculated for $[C_{33}H_{98}P_{14}Pt_4]$ (M_W = 1709.1): C 24.26, H 5.70; found: C 24.19, H 5.83.

Syntheses of diplatinum A-Frame boranediyl complexes

*General procedure **A***

In a vial one equivalent of the relevant dihaloborane was added to a benzene solution (0.7 mL) of **2**. The mixture was shaken, causing the immediate precipitation of an orange or yellow solid. After filtration the solid was recrystallised from CH_2Cl_2/pentane.

*General procedure **B***

In a vial one equivalent of the relevant trihaloborane dimethylsulfide adduct was added to a benzene solution (0.7 mL) of **2**. The mixture was shaken, causing the immediate precipitation of a yellow solid. After filtration the solid was recrystallised from CH_2Cl_2/pentane.

*General procedure **C***

In a vial two equivalents of the relevant dihaloborane were added to a benzene solution (0.7 mL) of **1**. The mixture was shaken, causing the immediate precipitation of an orange or yellow solid. After filtration the solid was recrystallised from CH_2Cl_2/pentane.

***Note:** the isolated A-Frame boranediyl complexes decomposed in solution or under reduced pressure.*

[$Pt_2Cl_2(\mu$-BDur)(μ-dmpm$)_2$], 4-Cl^{Dur}

A) Complex **2** (40.0 mg, 47.1 µmol) and 1.0 equivalent of BCl_2Dur (10.1 mg, 47.1 µmol) yielded **4-Cl^{Dur}** as a yellow solid (12.7 mg, 14.1 µmol, 82%). ^{1}H NMR (500.1 MHz, CD_2Cl_2): δ = 7.24 (s, 1H, Dur-CH), 3.20 (s, 6H, Dur-CH_3), 2.29 (s, 6H, Dur-CH_3), 1.89-2.03 (m, 2H, PCH_2), 1.78-1.84 (m, 12H, PCH_3), 1.66-1.74 (m, 2H; PCH_2), 1.41-1.33 (br. + satellites, 12H, $^3J_{HPt}$ = 40.0 Hz, PCH_3) ppm. ^{13}C{^{1}H} NMR (125.8 MHz, CD_2Cl_2): δ = 148.8 (br, BC_{Dur}) 136.6 (*m*-Dur-*C*), 134.9 (*p*-Dur), 30.8-29.9 (m, PCH$_2$), 25.4 (Dur-CH$_3$), 21.3 (Dur-CH$_3$), 14.1-14.5 (m, PCH$_3$) ppm. ^{31}P{^{1}H} NMR (162.2 MHz, CD_2Cl_2): δ = –11.6 (s + higher order satellites, $^1J_{\mathrm{P\text{-}Pt}}$ = 3544 Hz, $^3\mathrm{J}_{\mathrm{P\text{-}Pt}}$ = 244 Hz, $Q = J_{\mathrm{P1\text{-}P2}} + J_{\mathrm{P1\text{-}P3}}$ = 57 Hz) ppm. ^{11}B{^{1}H} NMR (160.5 MHz, CD_2Cl_2): δ = 97 (br s, fwmh ≈ 2310 Hz) ppm. ^{195}Pt{^{1}H} NMR (86.1 MHz, CD_2Cl_2): δ = −3687 (v. br t, $^1J_{\mathrm{P\text{-}Pt}}$ = 3500 Hz) ppm. Elemental analysis (%) calculated for [$C_{20}H_{41}BCl_2P_4Pt_2$] (M_W = 877.3): C 27.38, H 4.71; found: C 27.99, H 4.75.

[Pt_2Cl_2(*μ*-BTip)(*μ*-dmpm)$_2$], 4-Cl$^{\mathbf{Tip}}$

A) Complex **2** (15.0 mg, 17.6 µmol) and 1.0 equivalent of BCl_2Tip (5.03 mg, 17.6 µmol) yielded **4-Cl$^{\mathbf{Tip}}$** as a yellow solid (11.9 mg, 12.5 µmol, 71%). ^{1}H NMR (500.1 MHz, CD_2Cl_2): δ = 7.06 (s, 2H, *m*-Tip-CH_2), 5.14-5.24 (m, 2H, *o*-Tip-C*H*), 2.81-2.89 (m, 1H, *p*-Tip-C*H*), 1.93-2.27 (m, 2H, *P*CH_2), 1.86 (br. + satellites, 12H, $^3J_{HPt}$ = 27.0 Hz, *P*CH_3), 1.55-1.61 (m, 2H, *P*CH_2), 1.36 (br. + satellites, 12H, $^3J_{HPt}$ = 37.0 Hz, *P*CH_3), 1.28-1.29 (d, $^1J_{HH}$ = 6.88 Hz, 12H, *o*-Tip-CH_3), 1.24-1.25 (d, $^1J_{HH}$ = 6.98 Hz, 6H, *p*-Tip-CH_3) ppm. ^{13}C{^{1}H} NMR (125.8 MHz, CD_2Cl_2): δ = 152.4 (BC_{Tip}), 150.6 (*o*-Tip-*C* + *p*-Tip-*C*), 122.4 (*m*-Tip-*C*H), 36.2 (br. + satellites, *o*-Tip-*C*H), 36.0 (s, *p*-Tip-*C*H), 30.0-30.9 (m, P*C*H_2), 25.8 (*o*-Tip-*C*H_3), 23.7 (*p*-Tip-*C*H_3), 14.4-14.8 (m, P*C*H_3) ppm. *Note: the ^{13}C NMR resonances of the dmpm ligands appear as complex multiplets due to coupling with the various ^{31}P nuclei of the molecules.* ^{11}B{^{1}H} NMR (160.5 MHz, CD_2Cl_2): δ = 96 (br s, fwmh ≈ 2350 Hz) ppm. ^{31}P{^{1}H} NMR (202.5 MHz, CD_2Cl_2): δ = −11.3 (s + higher order satellites, $^1J_{\mathrm{P\text{-}Pt}}$ = 3551 Hz, $^3J_{\mathrm{P\text{-}Pt}}$ = 242 Hz, Q = $^2J_{\mathrm{P1\text{-}P2}}$ + $^2J_{\mathrm{P1\text{-}P3}}$ = 49 Hz) ppm. Elemental analysis (%) calculated for [$C_{25}H_{51}BCl_2P_4Pt_2$] (M_W = 947.46): C 31.69, H 4.43; found: C 31.12, H 5.30.

[Pt_2Cl_2(*μ*-$BNPh_2$)(*μ*-dmpm)$_2$], 4-Cl$^{\mathbf{NPh2}}$

A) Complex **2** (100 mg, 118 µmol) and 1.0 equivalent of BCl_2NPh_2 (29.4 mg, 118 µmol) yielded **4-Cl$^{\mathbf{NPh2}}$** as an orange solid (22.2 mg, 24.4 µmol, 21%). ^{1}H NMR (400.1 MHz, CD_2Cl_2): δ = 7.62 (d, $^3J_{\mathrm{HH}}$ = 7.48 Hz, 4H, *o*-Ph-C*H*), 7.26 (br. + satellites, 4H, $^3J_{HPt}$ = 27.9 Hz, *m*-Ph-C*H*), 7.36 (br. + satellites, 2H, $^3J_{HPt}$ = 36.4 Hz, *p*-Ph-C*H*), 1.94-2.20 (dm, 2H, $^2J_{HH}$ = 8.7 Hz, *P*CH_2), 1.80-1.86 (m, 2H, *P*CH_2), 1.69 (br. + satellites, $^3J_{\mathrm{HPt}}$ = 27 Hz, 12H, PCH_3), 1.31 (br. + higher order satellites, $^3J_{\mathrm{HPt}}$ = 38 Hz, 12H, PCH_3) ppm. ^{13}C{^{1}H} NMR (100.6 MHz, CD_2Cl_2, 297 K): δ = 153.18 (Ph-C_{N}), 128.83 (*m*-Ph-*C*H), 126.95 (*o*-Ph-*C*H), 124.24 (*p*-Ph-*C*H), 28.69-29.61 (m, P*C*H_2), 15.3-15.7 (m, P*C*H_3), 14.39-14.75 (m, P*C*H_3) ppm. ^{11}B{^{1}H} NMR (128.4 MHz, CD_2Cl_2): δ = 58 (br s, fwmh ≈ 2200 Hz) ppm. ^{31}P{^{1}H} NMR (162.0 MHz, CD_2Cl_2): δ = −6.7 (s + higher order satellites, $^1J_{\mathrm{P\text{-}Pt}}$ = 3415 Hz, $^3J_{\mathrm{P\text{-}Pt}}$ = 232 Hz, Q = $^2J_{\mathrm{P1\text{-}P2}}$ + $^2J_{\mathrm{P1\text{-}P3}}$ = 46 Hz) ppm. Elemental analysis (%) calculated for [$C_{22}H_{38}NBCl_2P_4Pt_2$] ($M_W$ = 912.33): C 28.96, H 4.20, N 1.54; found: C 27.89, H 4.18, N 1.37.

[Pt_2Cl_2(*μ*-BCl)(*μ*-dmpm)$_2$], 4-Cl$^{\mathbf{Cl}}$

A) Complex **2** (100 mg, 118 µmol) and 1.0 equivalent of 1M in hexane BCl_3 (13.8 mg, 118 µmol) yielded **4-Cl$^{\mathbf{Cl}}$** as a yellow solid (3.67 mg, 4.70 µmol, 20%).

B) 2 (20.0 mg, 23.51 µmol) and 1.0 equivalent of $Me_2S{\cdot}BCl_3$ (4.22 mg, 23.51 µmol) yielded **4-Cl^{Cl}** as a yellow solid (18.0 mg, 23.0 µmol, 98%). ^{1}H NMR (400.6 MHz, C_6D_6/CD_2Cl_2): δ = 1.36 (br. + satellites, 12H, $^3J_{HPt}$ = 25.1 Hz, PCH_3), 1.22-1.27 (m, 2H, PCH_2), 1.19 (br. + satellites, 12H, $^3J_{HPt}$ = 30.5 Hz, PCH_3), 0.92-1.11 (dm, 2H, $^2J_{HH}$ = 8.7 Hz, PCH_2) ppm. ^{13}C{^{1}H} NMR (100.6 MHz, C_6D_6/CD_2Cl_2): δ = 27.2-27.6 (m, PCH_2), 14.7 (br. + satellites, $^1J_{CP}$ = 20.7 Hz PCH_3), 13.2-13.6 (m, PCH_3) ppm. *Note: the ^{13}C NMR resonances of the dmpm ligands appear as complex multiplets due to coupling with the various ^{31}P nuclei of the molecules.* ^{11}B{^{1}H} NMR (128.5 MHz, C_6D_6/CD_2Cl_2): δ = 85 (br s, fwmh ≈ 2170 Hz) ppm. ^{31}P{^{1}H} NMR (162.2 MHz, C_6D_6/CD_2Cl_2): δ = –7.0 (s + higher order satellites, $^1J_{\text{P-Pt}}$ = 3328 Hz, $^3J_{\text{P-Pt}}$ = 230 Hz, $Q = {}^2J_{\text{P1-P2}} + {}^2J_{\text{P1-P3}} = 44$ Hz) ppm. Elemental analysis (%) calculated for $[C_{13}H_{32}BCl_3F_2P_4Pt_2]$ = [**4-Cl^{Cl}**$\cdot(C_6H_4F_2)_{0.5}$] (M_W = 779.6): C 18.21, H 3.76; found: C 18.20, H 3.64.

$[Pt_2Br_2(\mu\text{-BCy})(\mu\text{-dmpm})_2]$, 4-Br^{Cy}

A) Complex **2** (50.0 mg, 58.8 µmol) and 1.0 equivalent of BBr_2Cy (14.92 mg, 58.8 µmol) yielded **4-Br^{Cy}** as an orange solid (33.9 mg, 41.0 µmol, 70%). ^{1}H{^{31}P} NMR (500.1 MHz, CD_2Cl_2): δ = 2.63-2.68 (m, 2H, *p*-Cy-C*H*$_2$), 2.23-1.90 (m, 2H PC*H*$_2$), 1.89-1.65 (m, 28H, *o*-Cy-C*H*$_2$ + PC*H*$_3$), 1.47-1.39 (d, 2H, $^3J_{\text{HPt}}$ = 14 Hz, PC*H*$_2$), 1.37-1.16 (m, 5H, *m*-Cy-C*H*$_2$ + Cy-C*H*) ppm. ^{13}C{^{1}H} NMR (125.8 MHz, CD_2Cl_2): δ = 35.2-35.5 (m, P*C*H$_2$ + Cy-*C*H$_2$), 28.7 (Cy-*C*H$_2$), 27.4-28.2 (m, *C*H$_2$, Cy-*C*H$_2$), 26.9 (Cy-*C*H$_2$), 15.5-15.9 (m, P*C*H$_3$) ppm. ^{11}B{^{1}H} NMR (160.5 MHz, CD_2Cl_2): δ = 105 (br s, fwmh ≈ 2400 Hz) ppm. ^{31}P{^{1}H} NMR (162.0 MHz, CD_2Cl_2): δ = −7.4 (s + higher order satellites, $^1J_{\text{P-Pt}}$ = 3440 Hz, $^3J_{\text{P-Pt}}$ = 201 Hz, $Q = {}^2J_{\text{P1-P2}} + {}^2J_{\text{P1-P3}} = 55$ Hz) ppm. Elemental analysis (%) calculated for $[C_{16}H_{39}BBr_2P_4Pt_2]$ (M_W = 916.2): C 20.98, H 4.29; found: C 21.12, H 4.28.

$[Pt_2Br_2(\mu\text{-BMes})(\mu\text{-dmpm})_2]$, 4-Br^{Mes}

A) Complex **2** (15.0 mg, 17.6 µmol) and 1.0 equivalent of BBr_2Mes (5.09 mg, 17.6 µmol) yielded **4-Br^{Mes}** as an orange solid (15.1 mg, 10.6 µmol, 60%).

C) Complex **1** (40.0 mg, 51.7 µmol) and 2.0 equivalents of BBr_2Mes (29.9 mg, 103 µmol) yielded **4-Br^{Mes}** as an orange solid (24.1 mg, 25.3 µmol, 49%). ^{1}H NMR (500.1 MHz, CD_2Cl_2): δ = 6.96 (s, 1H, Mes-C*H*), 3.15 (s, 6H, Mes-C*H*$_3$), 2.19 (s, 3H, Mes-C*H*$_3$), 1.95 (dm, 2H, $^2J_{HH}$ = 4.3 Hz PC*H*$_2$), 1.88 (br. + satellites, 12H, $^3J_{\text{HPt}}$ = 34 Hz, PC*H*$_3$), 1.42 (br.+ satellites, 12H, $^3J_{\text{HPt}}$ = 34 Hz, $^3J_{\text{HPt}}$ = 34 Hz, PC*H*$_3$), 1.22-1.27 (m, 2H, PC*H*$_2$) ppm. ^{13}C{^{1}H} NMR (125.8 MHz, CD_2Cl_2): δ = 142.0 (BC_{Mes}), 141.2 (Mes-*C*), 130.6 (*m*-Mes-*C*H), 29.9 (br. + satelittes, $^2J_{\text{CPt}}$ =

31 Hz, PCH_2), 29.6 (*m*-Dur-CH_3), 21.6 (*p*-Dur-CH_3), 16.0-15.7 (m, PCH_3), 14.9-14.6 (m, PCH_3) ppm. $^{11}B\{^1H\}$ NMR (160.5 MHz, CD_2Cl_2): δ = 97 (br s, fwmh ≈ 2250 Hz) ppm. $^{31}P\{^1H\}$ NMR (202.5 MHz, CD_2Cl_2): δ = −13.3 (s + higher order satellites, $^1J_{Pt1\text{-}P1}$ = 3506 Hz, $^3J_{P\text{-}Pt}$ = 233 Hz, Q = $^2J_{P1\text{-}P2}$ + $^2J_{P1\text{-}P3}$ = 54 Hz) ppm. Elemental analysis (%) calculated for [$C_{19}H_{39}BBr_2P_4Pt_2$] (M_W = 952.2): C 23.97, H 4.13; found: C 24.26, H 4.15. *Note: Single crystals of two types of dmpm-BMesBr$_2$ byproducts were isolated during fractional recrystallisation: the linear dmpm-bis(borane) adduct (μ-dmpm)(BMesBr$_2$)$_2$ was formed, in which each phosphine moiety coordinates one borane, and a chelating dmpm-boronium adduct with a bromide counteranion, [(η^2-dmpm)BMesBr]Br (δ_{11B} = –3.5 (br) ppm; δ_{31P} = –6.1 (br) ppm).*

[Pt$_2$Br$_2$(*μ*-BDur)(*μ*-dmpm)$_2$], 4-Br^{Dur}

C) Complex **1** (40.0 mg, 51.7 µmol) and 2.0 equivalents of BBr_2Dur (31.4 mg, 103 µmol) yielded **4-Br^{Dur}** as an orange solid (22.0 mg, 22.7 µmol, 44%). NMR-spectroscopic data matched that from the literature, where **4-Br^{Dur}** was obtained through route **A)**.[8]

[Pt$_2$I$_2$(*μ*-BI)(*μ*-dmpm)$_2$], 4-I^I

A) Complex **2** (20.0 mg, 23.5 µmol) and 1.0 equivalent of BI_3 (9.20 mg, 23.5 µmol) yielded **4-I^I** as a red solid (5.21 mg, 4.94 µmol, 21%). ^1H NMR (400.6 MHz, CD_2Cl_2): δ = 2.26-2.07 (m, 4H PCH_2), 1.87 (br + satellites, 12H, *P*CH_3), 1.76 (br + satellites, 12H, PCH_3) ppm. $^{13}C\{^1H\}$ NMR (100.7 MHz, CD_2Cl_2): δ = 21.6-21.2 (m, 2C, PCH_2), 17.3-17.0 (m, 4C, *P*CH_3), 16.1-15.6 (m, 4C, *P*CH_3) ppm. $^{31}P\{^1H\}$ NMR (162.0 MHz, CD_2Cl_2): δ = −15.5 (s + higher order satellites, $^1J_{P\text{-}Pt}$ = 3214 Hz, $^3J_{P\text{-}Pt}$ = 195 Hz, Q = $^2J_{P1\text{-}P2}$ + $^2J_{P1\text{-}P3}$ = 44 Hz) ppm. $^{11}B\{^1H\}$ NMR (128.5 MHz, CD_2Cl_2): δ = 80 (br s, fwmh ≈ 2730 Hz) ppm. Elemental analysis (%) calculated for [$C_{10}H_{28}BI_3P_4Pt_2$] = [**4-I^I**] (M_W = 1053.9): C 11.4, H 2.68; found: C 11.92, H 2.78.

[(μ-dmpm)PtI]$_2$, 6-I

A small crop of colourless crystals of **6-I** suitable for X-ray crystallographic analysis was isolated from the decomposition of **4-I^I**. The NMR data fits the literature report of **6-I**.[9] $^{31}P\{^1H\}$ NMR (162.0 MHz, CD_2Cl_2): δ = –31.4 (s + higher order satellites, $^1J_{P\text{-}Pt}$ = 2629 Hz, $^2J_{P\text{-}Pt}$ = 141 Hz, Q = $^2J_{P1\text{-}P2}$ + $^2J_{P1\text{-}P3}$ = 73 Hz). In solution **6-I** underwent disproportionation to **7-I** and an unknown, insoluble Pt(0) compound.

Independent synthesis of $[Pt_2I_4(\mu\text{-dmpm})_2]$, 7-I

In a vial two equivalents of I_2 (36.0 mg, 141.8 µmol) were added to a benzene solution (0.7 mL) of **2** (60.3 mg, 70.9 µmol). The mixture was shaken, causing the immediate precipitation of a red solid. After filtration the solid was recrystallised from CH_2Cl_2/pentane. Yielded **7-I** as a red crystalline solid (59.8 mg, 51.06 µmol, 73%). ^{1}H NMR (400.6 MHz, CD_2Cl_2): δ = 3.31 (s, 4H, PCH_2), 2.24 (s, 24H, PCH_3) ppm. $^{13}C\{^1H\}$ NMR (125.8 MHz, CD_2Cl_2): δ = 39.5 (PCH_2), 19.6 (PCH_3) ppm. $^{31}P\{^1H\}$ NMR (162.0 MHz, CD_2Cl_2): δ = –34.4 (s + higher order satellites, $^1J_{P\text{-}Pt}$ = 2258 Hz, $^2J_{P1\text{-}P2} + {}^2J_{P1\text{-}P3}$ = 49 Hz) ppm. Elemental analysis (%) calculated for $[C_{10}H_{28}I_4P_4Pt_2]$ (M_W = 1170.01): C 10.27, H 2.41; found: C 10.34, H 2.42.

Synthesis and decomposition of diplatinum A-frame diborane-1,2-diyl complexes

$[Pt_2Cl_2(\mu\text{-}B_2(NMe_2)_2)(\mu\text{-dmpm})_2]$, 5-Cl^{NMe2}

In a vial one equivalent of $B_2Cl_2(NMe_2)_2$ (5.09 mg, 17.6 µmol) was added to a benzene solution (0.7 mL) of **2** (15.0 mg, 17.6 µmol). The mixture was shaken, causing the immediate precipitation of an orange solid. After filtration the solid was recrystallised from CH_2Cl_2/pentane, yielding **5-Cl^{NMe2}** as an orange solid (15.3 mg, 16.1 µmol, 91%). ^{11}B NMR (128.5 MHz, CD_2Cl_2): δ = 57 (br s, 1110 Hz) ppm. $^{31}P\{^1H\}$ NMR (162.0 MHz, CD_2Cl_2): δ = –10.7 (br s, $^1J_{P\text{-}Pt}$ = 3399 Hz) ppm. *Note: Due to rapid decomposition in solution and in the solid state, only ^{11}B and $^{31}P\{^1H\}$ NMR data of **5-Cl^{NMe2}** could be acquired. Multiple attempts to obtain suitable elemental analysis data also failed.*

$[(\mu\text{-dmpm})PtCl]_2$, 6-Cl

A small amount of colourless **6-Cl** was isolated from the decomposition of **5-Cl^{NMe2}**. ^{1}H NMR (400.6 MHz, CD_2Cl_2): δ = 2.77-2.88 (m, 4H PCH_2), 1.71 (br + satellites, 12H, $^3J_{HPt}$ =14.2 Hz, PCH_3) ppm. $^{31}P\{^1H\}$ NMR (162.2 MHz, CD_2Cl_2): δ = –19.3 (s + higher order satellites, $^1J_{Pt1\text{-}P1}$ = 2654 Hz, $J_{Pt2\text{-}P1}$ = 149 Hz, $Q = J_{P1\text{-}P2} + J_{P1\text{-}P3}$ = 111 Hz) ppm. *Note: The compound was never isolated in sufficient quantities for further analysis.*

NMR spectra of new compounds

Figure S1. ^{1}H NMR spectrum of **1** in C_6D_6.

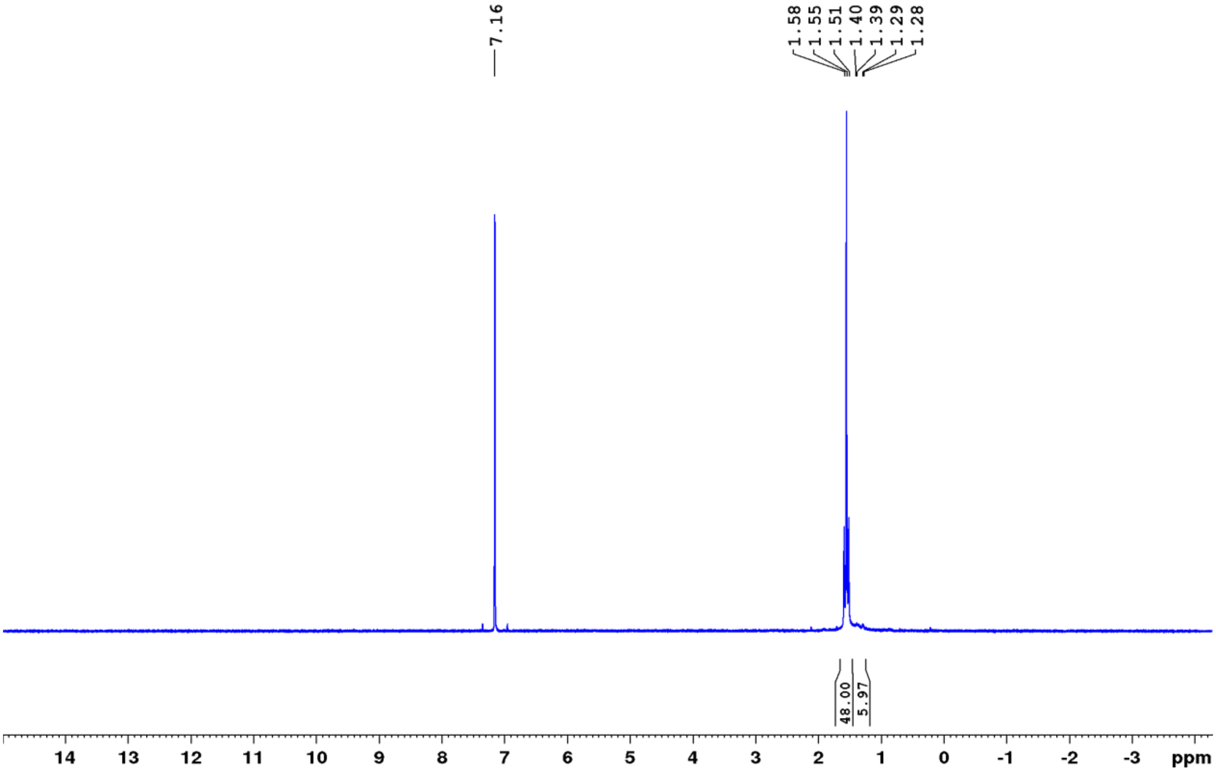

Figure S2. ^{13}C{^{1}H} NMR spectrum of **1** in C_6D_6.

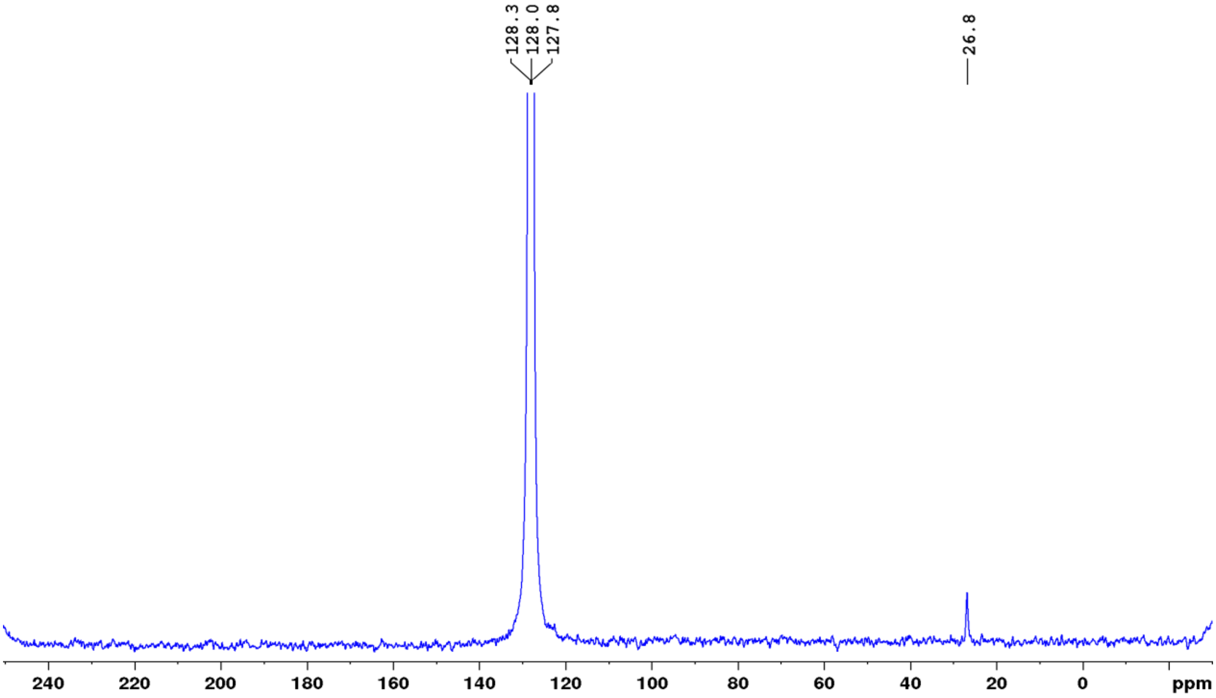

Figure S3. $^{31}P\{^1H\}$ NMR spectrum of **1** in C_6D_6.

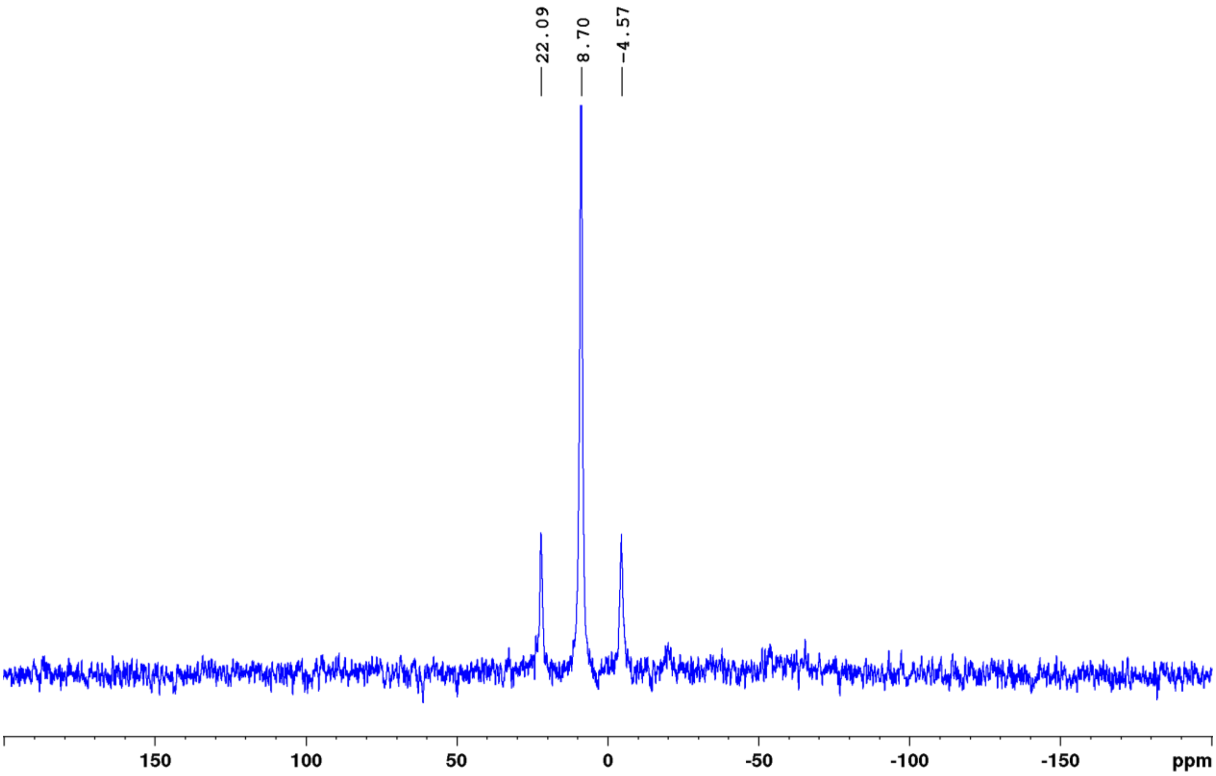

Figure S4. $^{31}P\{^1H\}$ NMR spectrum of the cluster decomposition product of **2**, [Pt_6(*μ*-dmpm)$_4$(*μ*-PMe_2)$_4$], in C_6D_6.

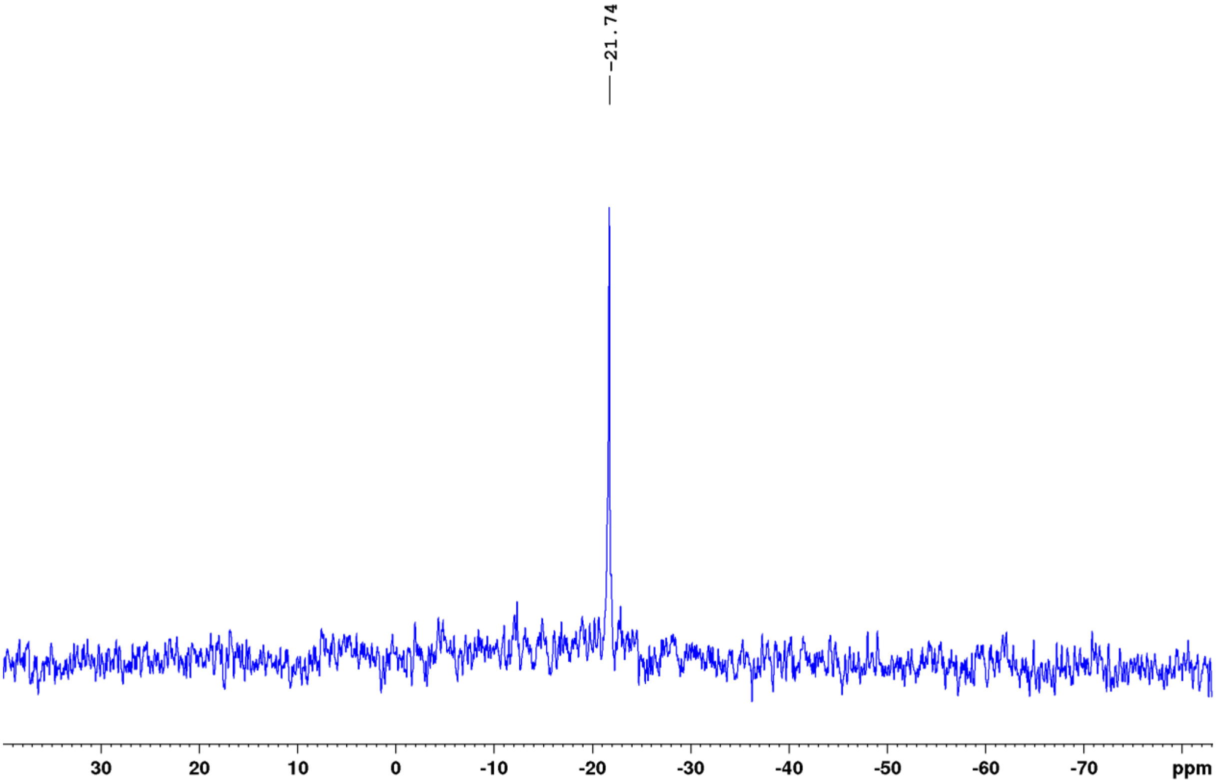

Figure S5. ^{1}H NMR spectrum of **4-Cl$^{\mathbf{Dur}}$** in CD_2Cl_2. The additional resonance at 0.88 ppm corresponds to residual pentane.

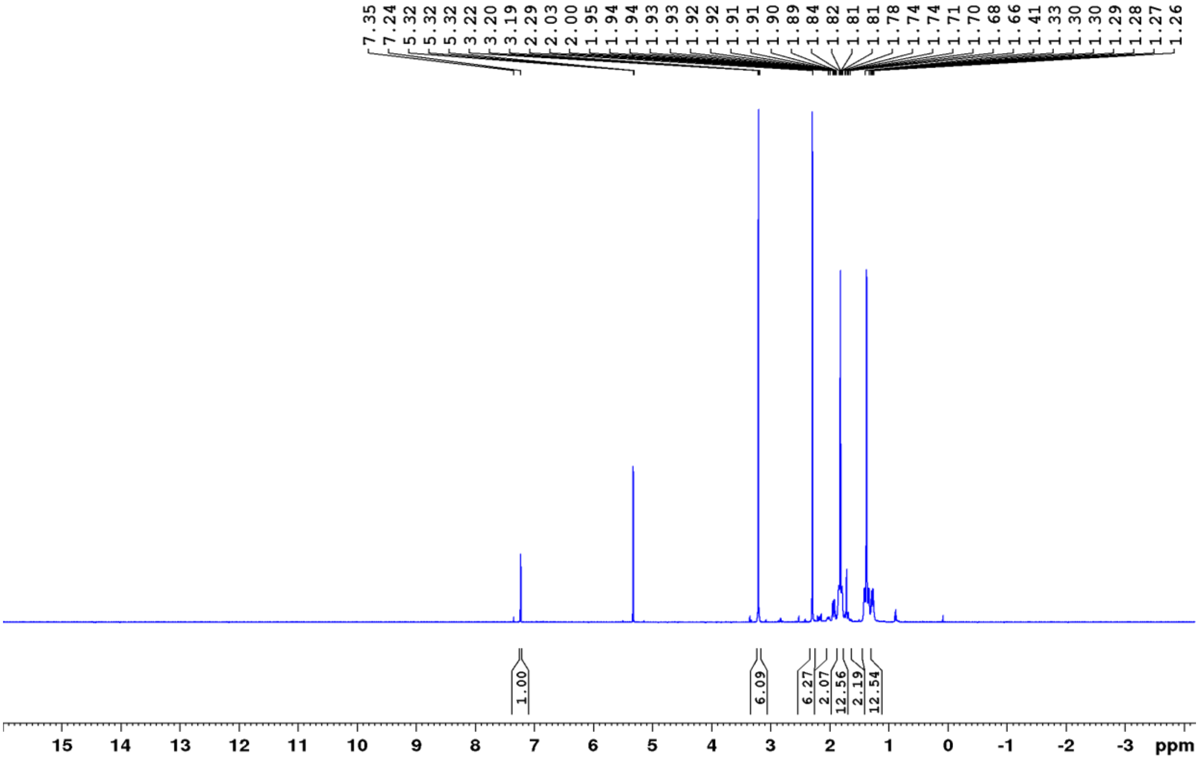

Figure S6. $^{13}C\{^1H\}$ NMR spectrum of **4-Cl$^{\mathbf{Dur}}$** in CD_2Cl_2.

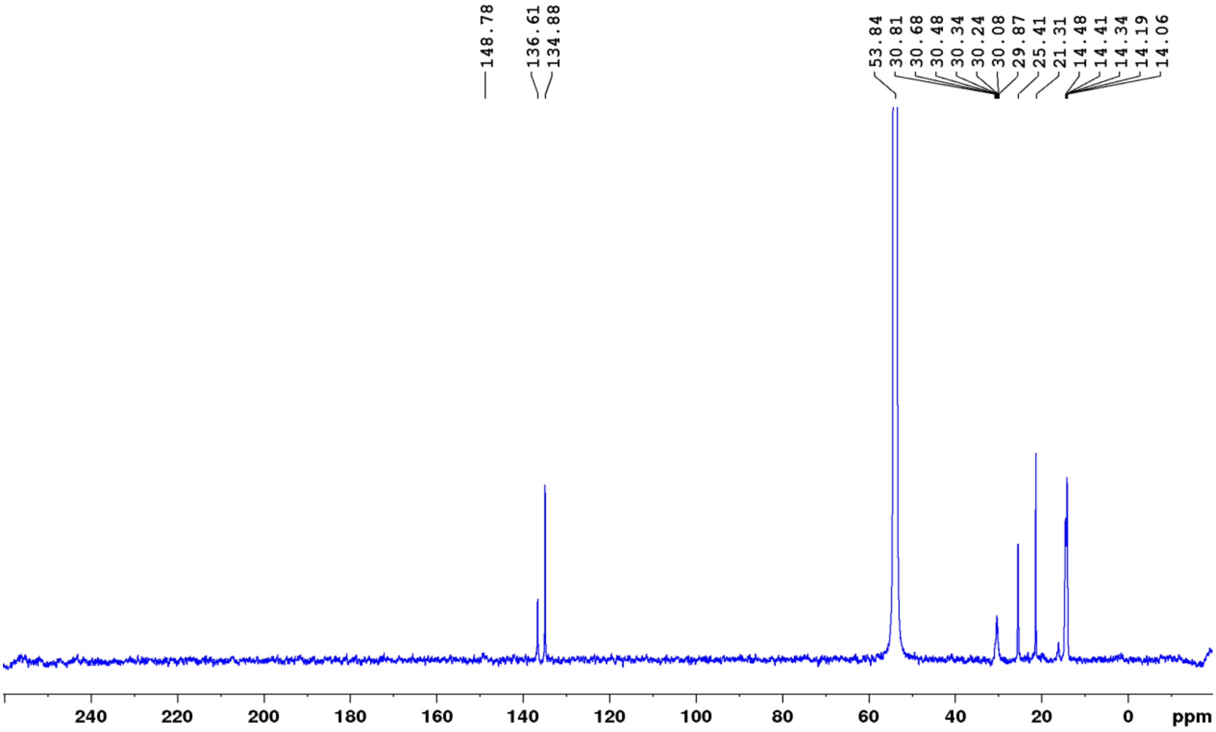

Figure S7. $^{11}B\{^{1}H\}$ NMR spectrum of **4-Cl^{Dur}** in CD_2Cl_2.

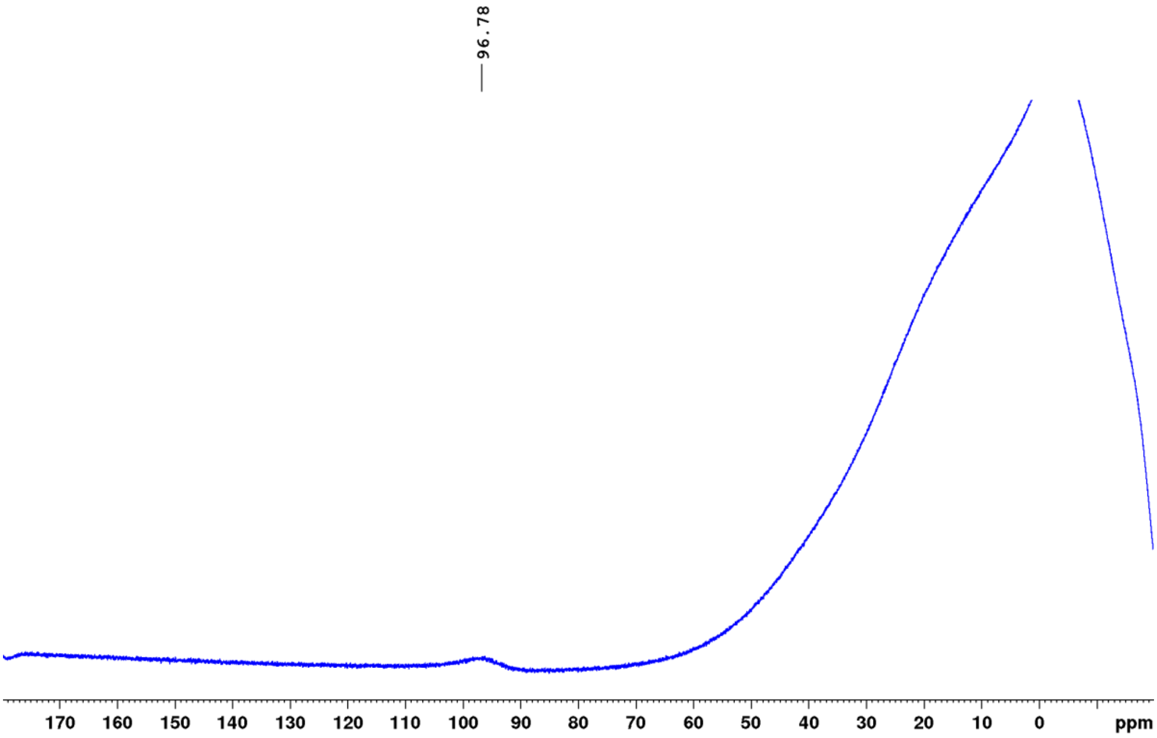

Figure S8. $^{31}P\{^{1}H\}$ NMR spectrum of **4-Cl^{Dur}** in CD_2Cl_2.

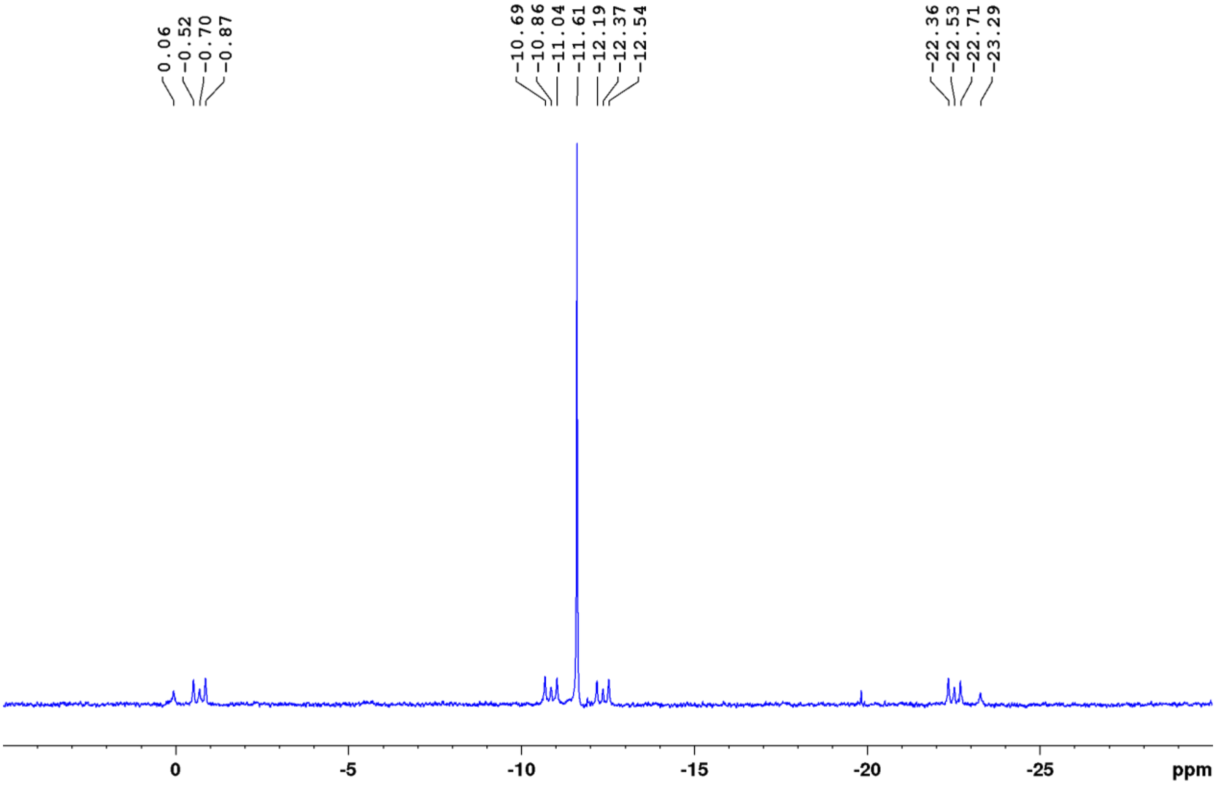

Figure S9. ^{195}Pt{^{1}H} NMR spectrum of **4-Cl$^{\mathbf{Dur}}$** in CD_2Cl_2.

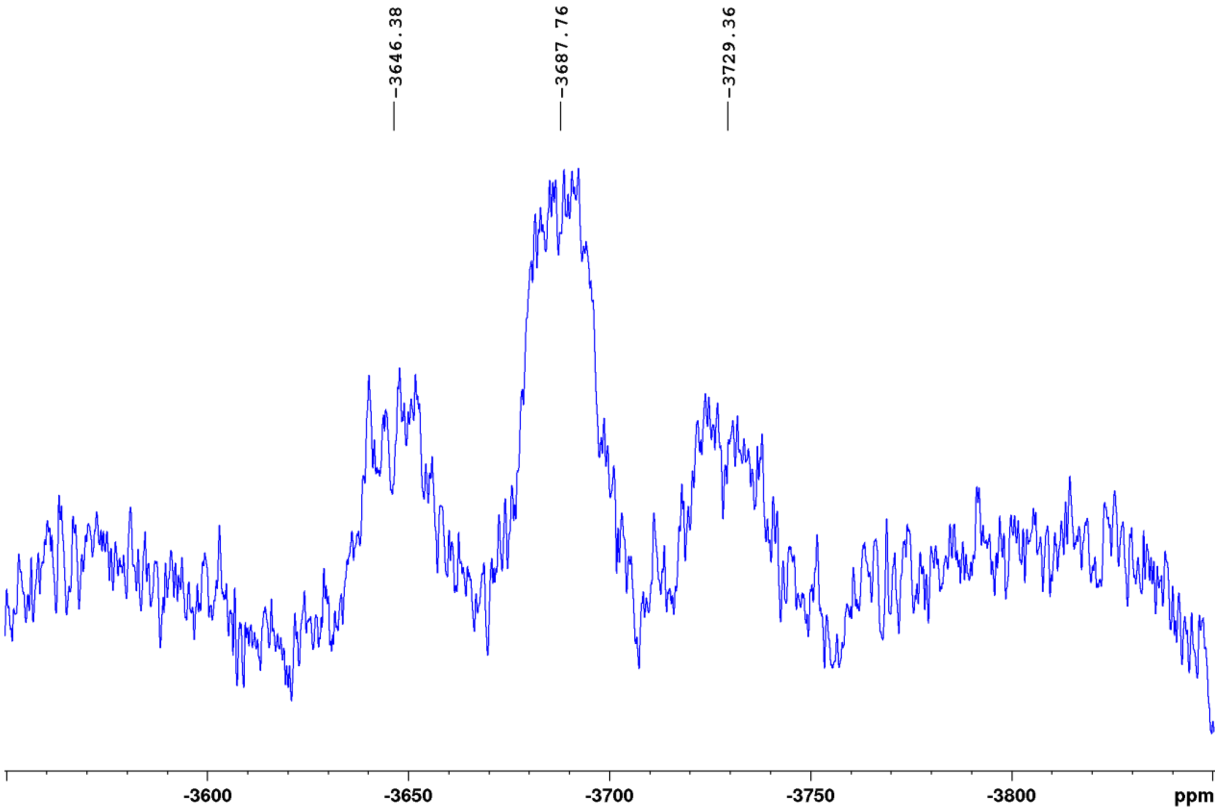

Figure S10. ^{1}H NMR spectrum of **4-Cl^{Tip}** in CD_2Cl_2. The additional resonance at 0.88 ppm corresponds to residual pentane.

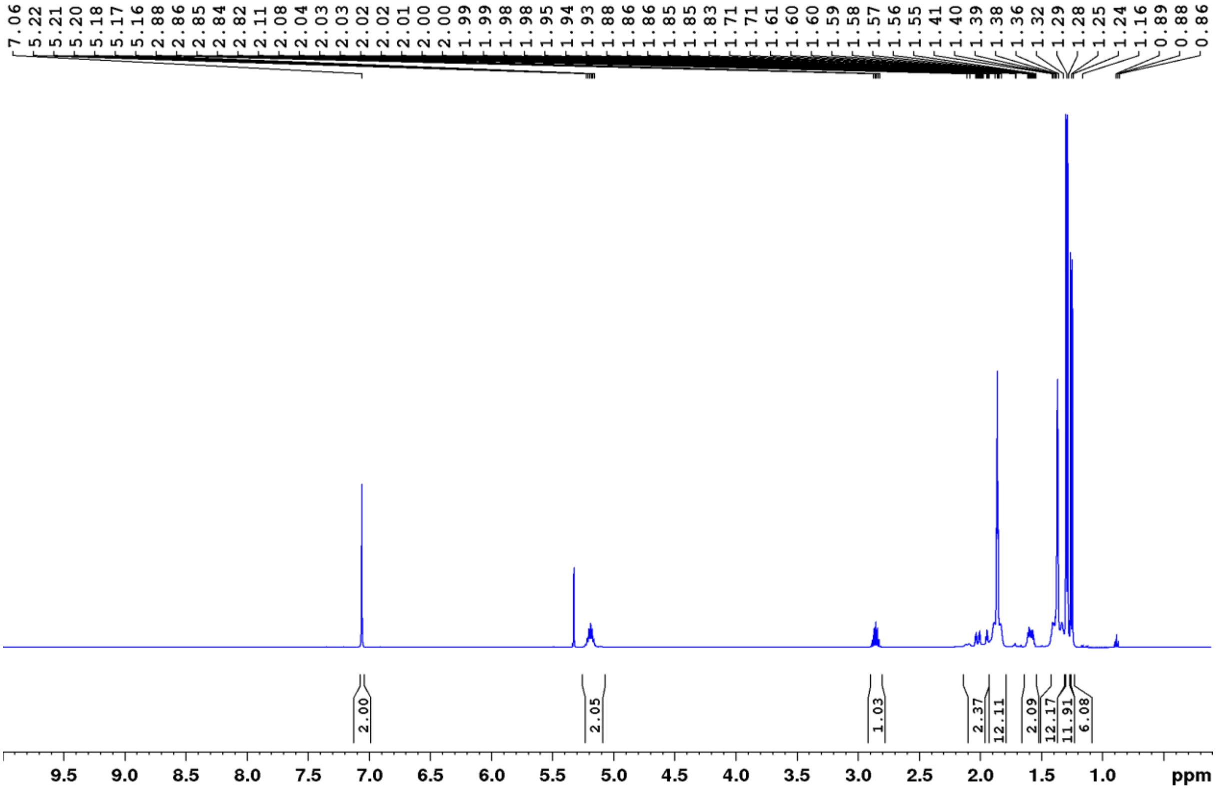

Figure S11. $^{13}C\{^1H\}$ NMR spectrum of **4-Cl^{Tip}** in CD_2Cl_2.

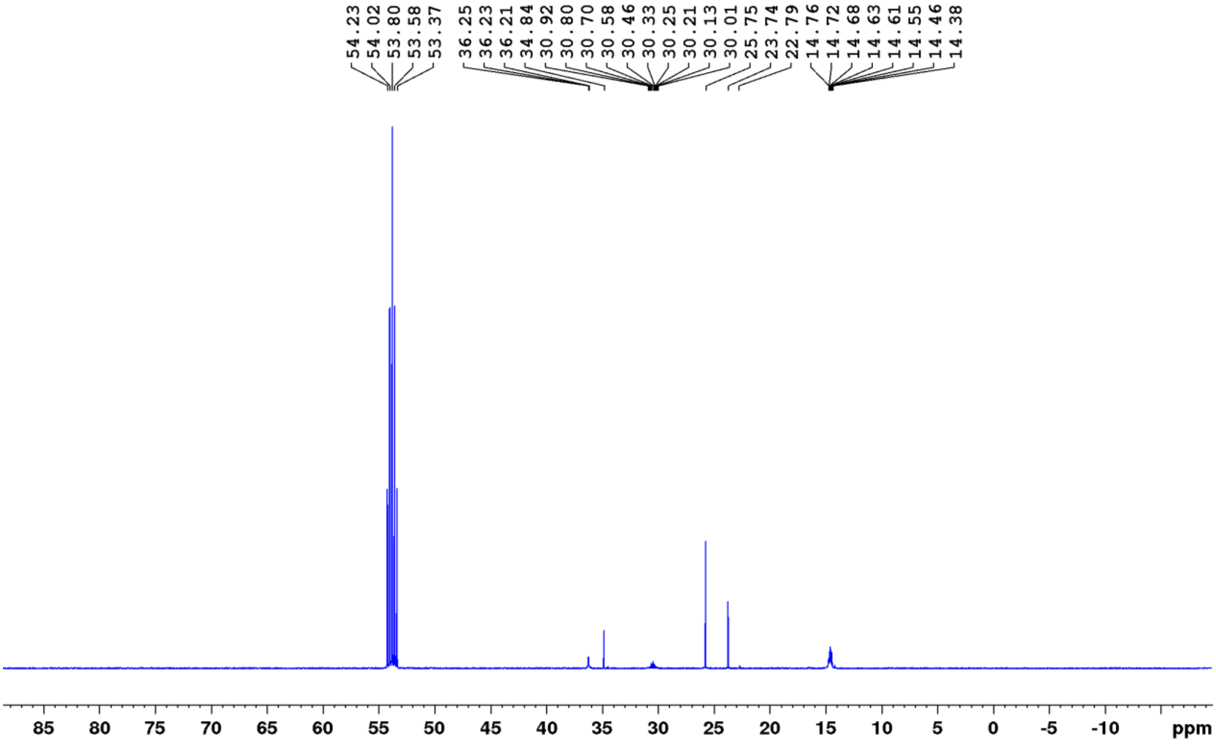

Figure S12. $^{11}B\{^1H\}$ NMR spectrum of **4-Cl^{Tip}** in CD_2Cl_2.

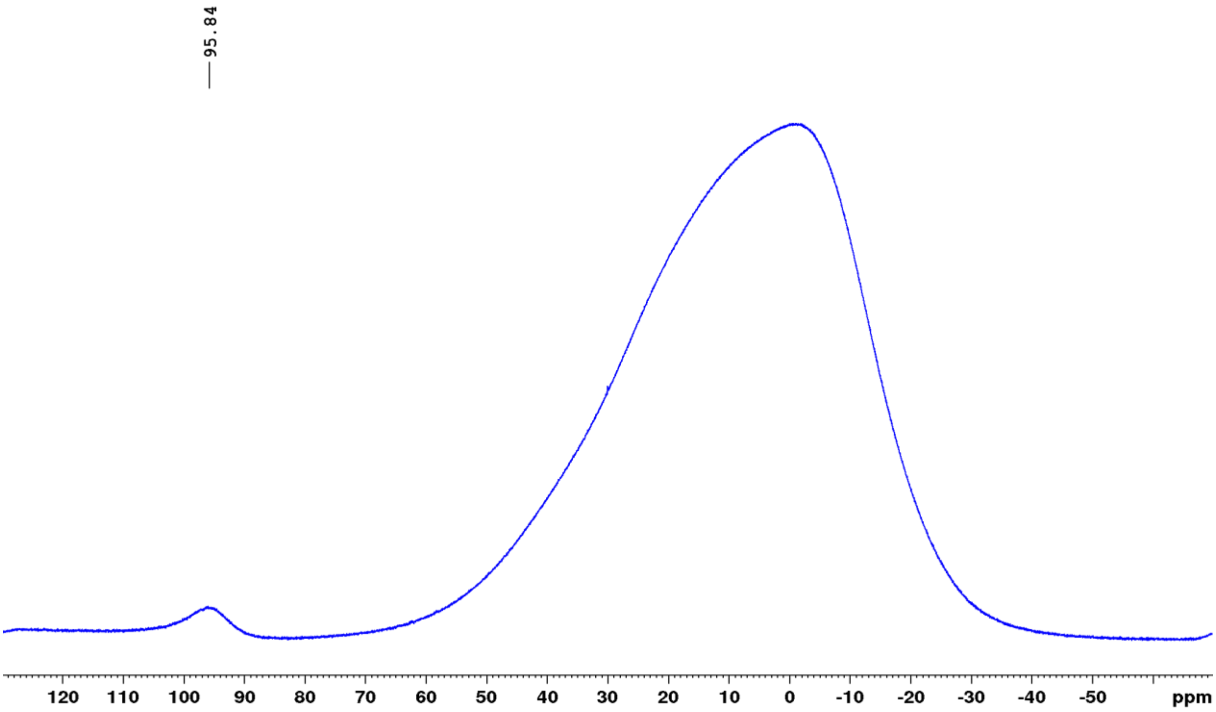

Figure S13. $^{31}P\{^1H\}$ NMR spectrum of **4-Cl^{Tip}** in CD_2Cl_2.

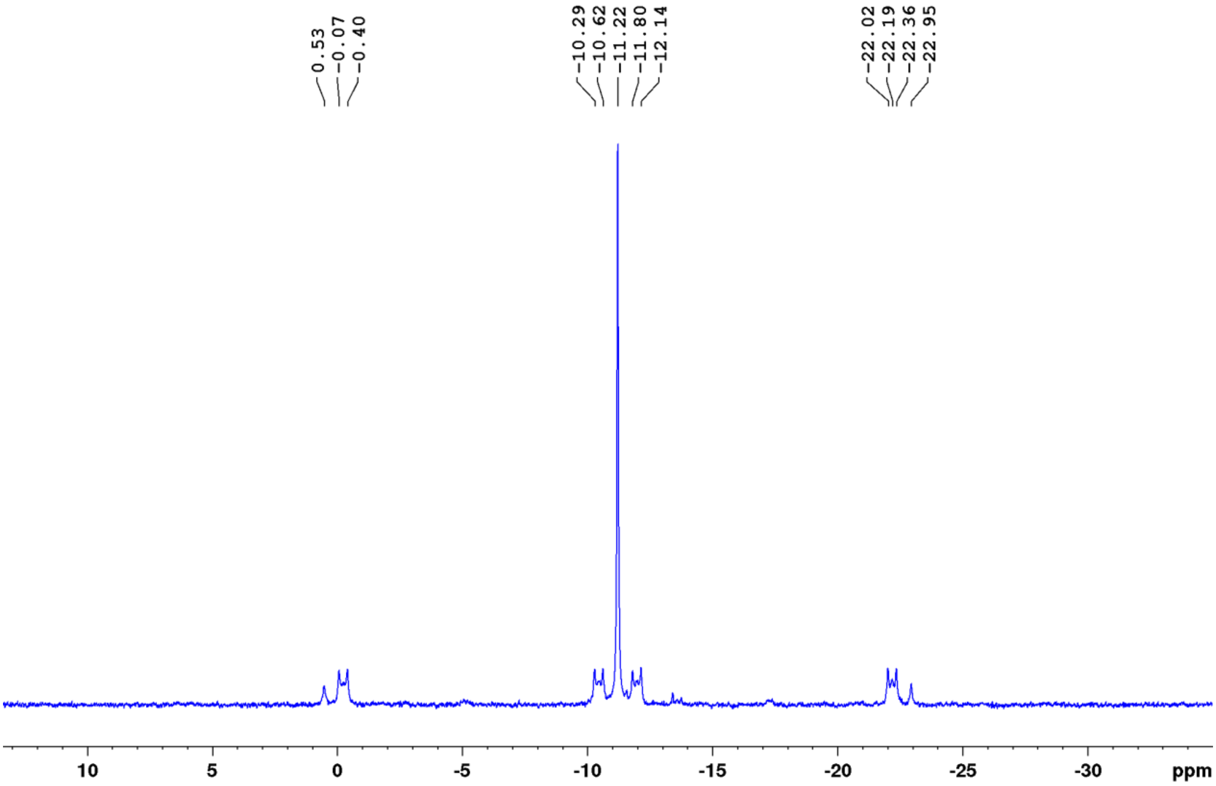

Figure S14. ^{1}H NMR spectrum of **4-Cl$^{\mathbf{NPh2}}$** in CD_2Cl_2.

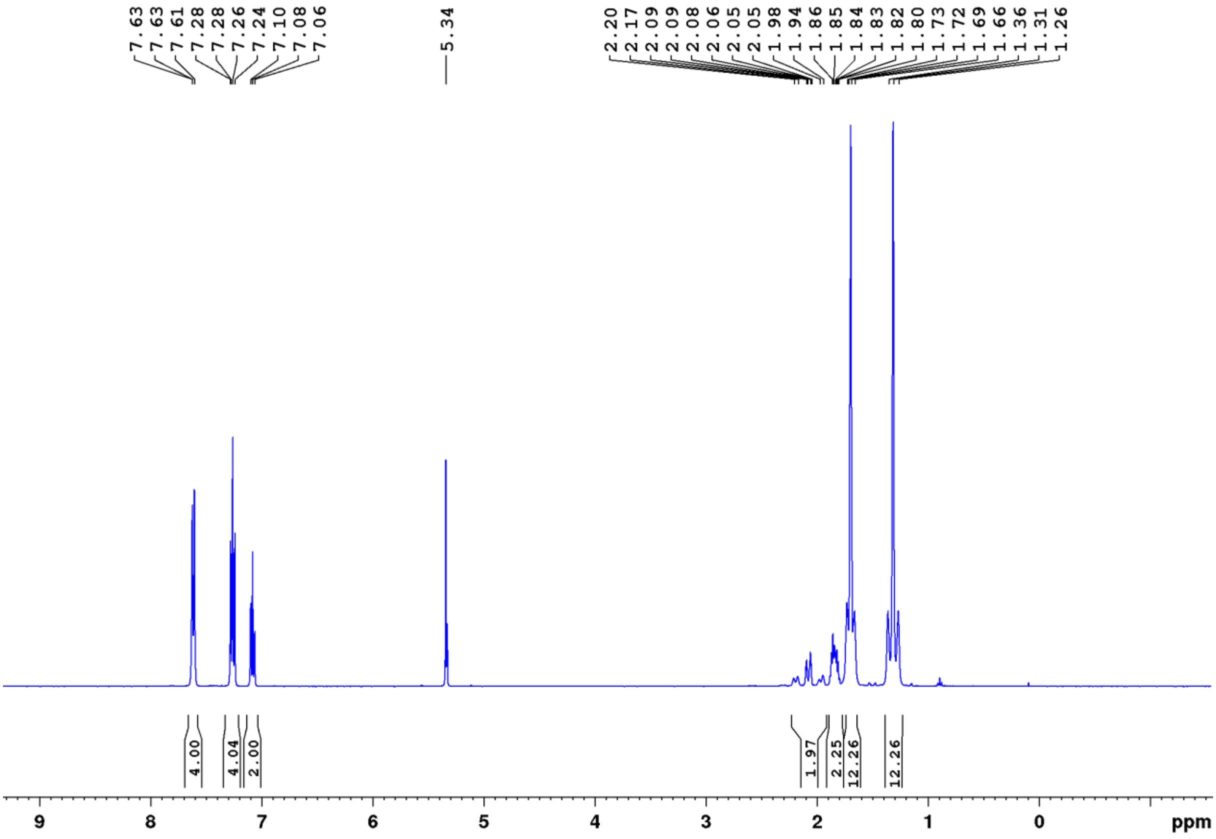

Figure S15. $^{13}C\{^1H\}$ NMR spectrum of **4-Cl$^{\mathbf{NPh2}}$** in CD_2Cl_2.

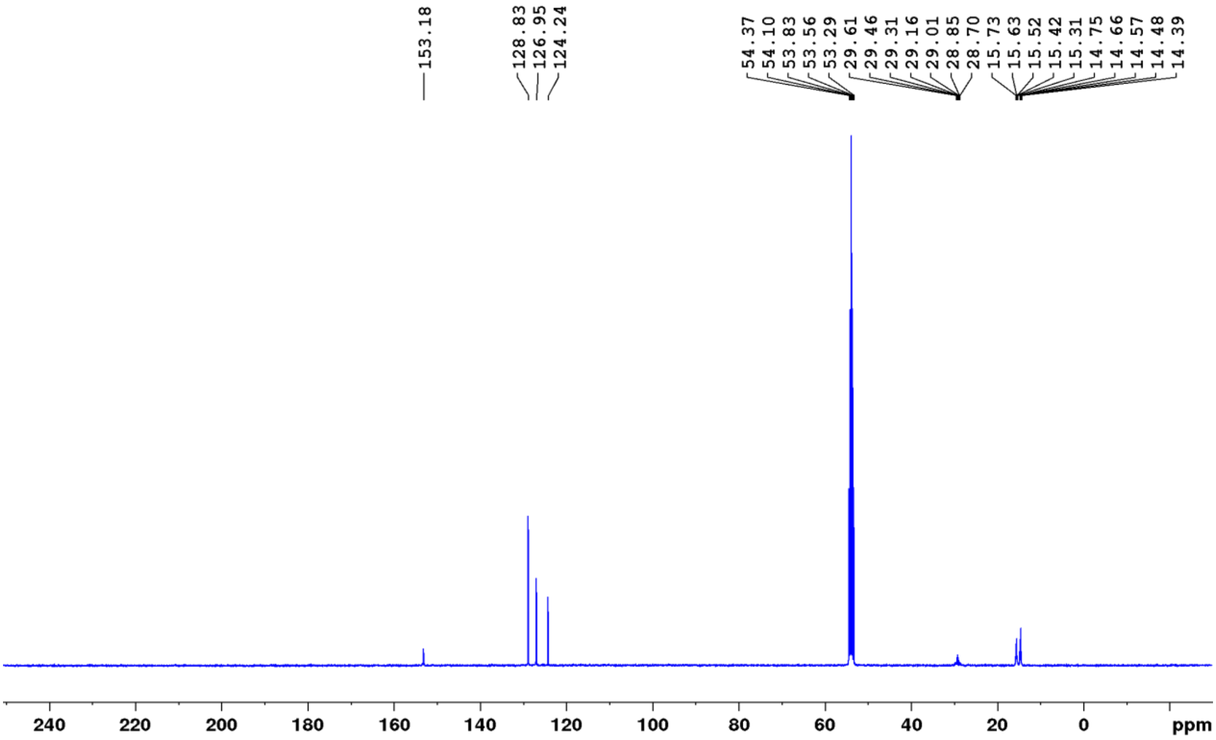

Figure S16. $^{11}B\{^1H\}$ NMR spectrum of **4-Cl^{NPh2}** in CD_2Cl_2.

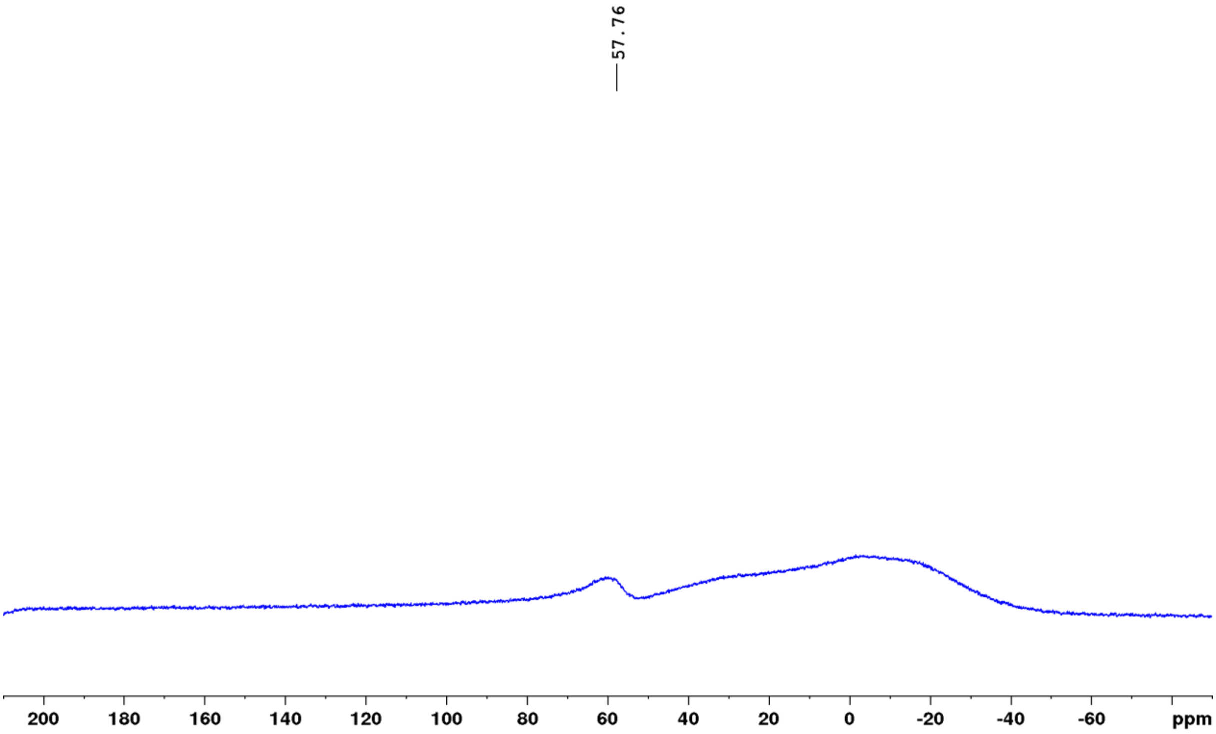

Figure S17. $^{31}P\{^1H\}$ NMR spectrum of **4-Cl^{NPh2}** in CD_2Cl_2.

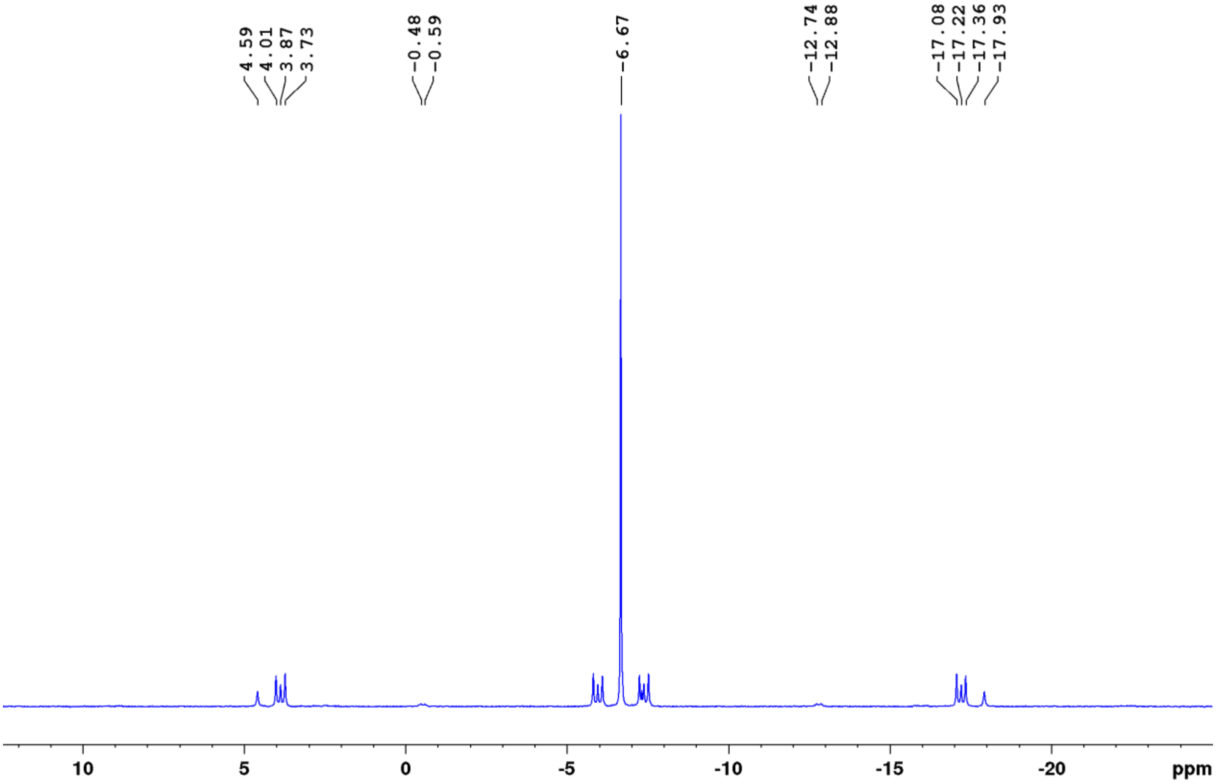

Figure S18. ^{1}H NMR spectrum of **4-Cl^{Cl}** in C_6D_6/CD_2Cl_2. The additional resonances at 1.23 and 0.86 ppm correspond to residual pentane.

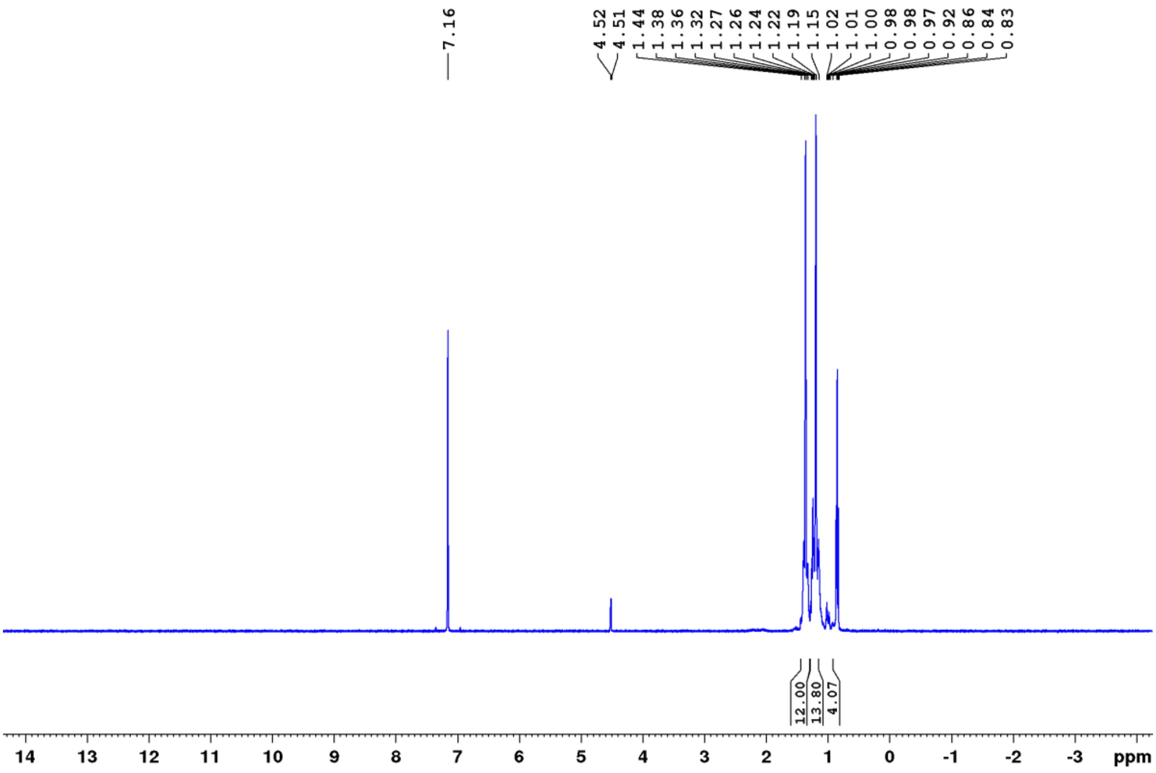

Figure S19. ^{13}C{^{1}H} NMR spectrum of **4-Cl^{Cl}** in C_6D_6/CD_2Cl_2. The additional resonances at 34.5, 22.7 and 14.3 ppm correspond to residual pentane.

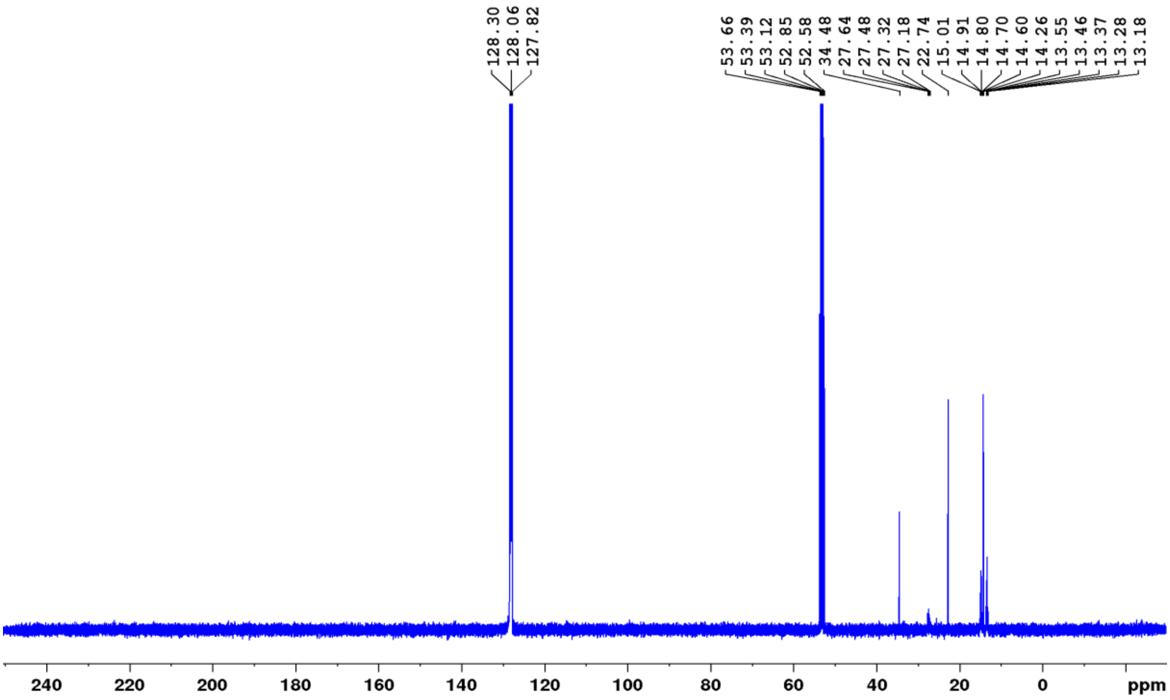

Figure S20. $^{11}B\{^{1}H\}$ NMR spectrum of **4-Cl^{Cl}** in C_6D_6/CD_2Cl_2.

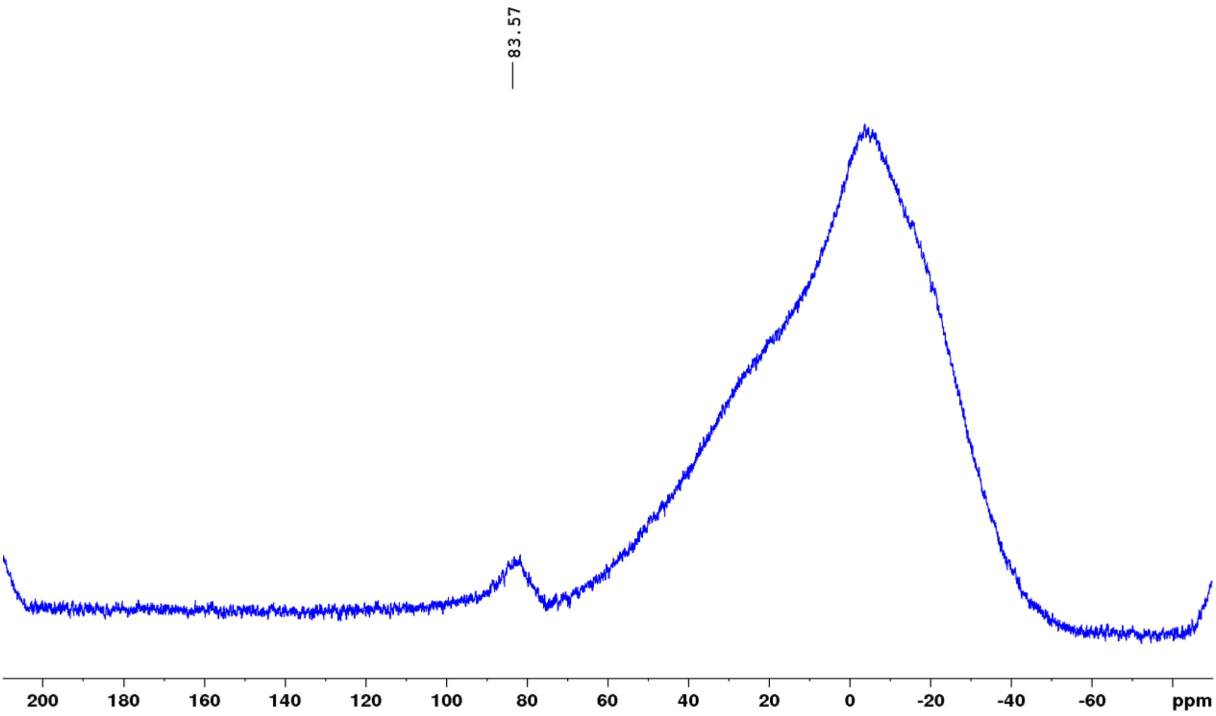

Figure S21. $^{31}P\{^{1}H\}$ NMR spectrum of **4-Cl^{Cl}** in C_6D_6/CD_2Cl_2.

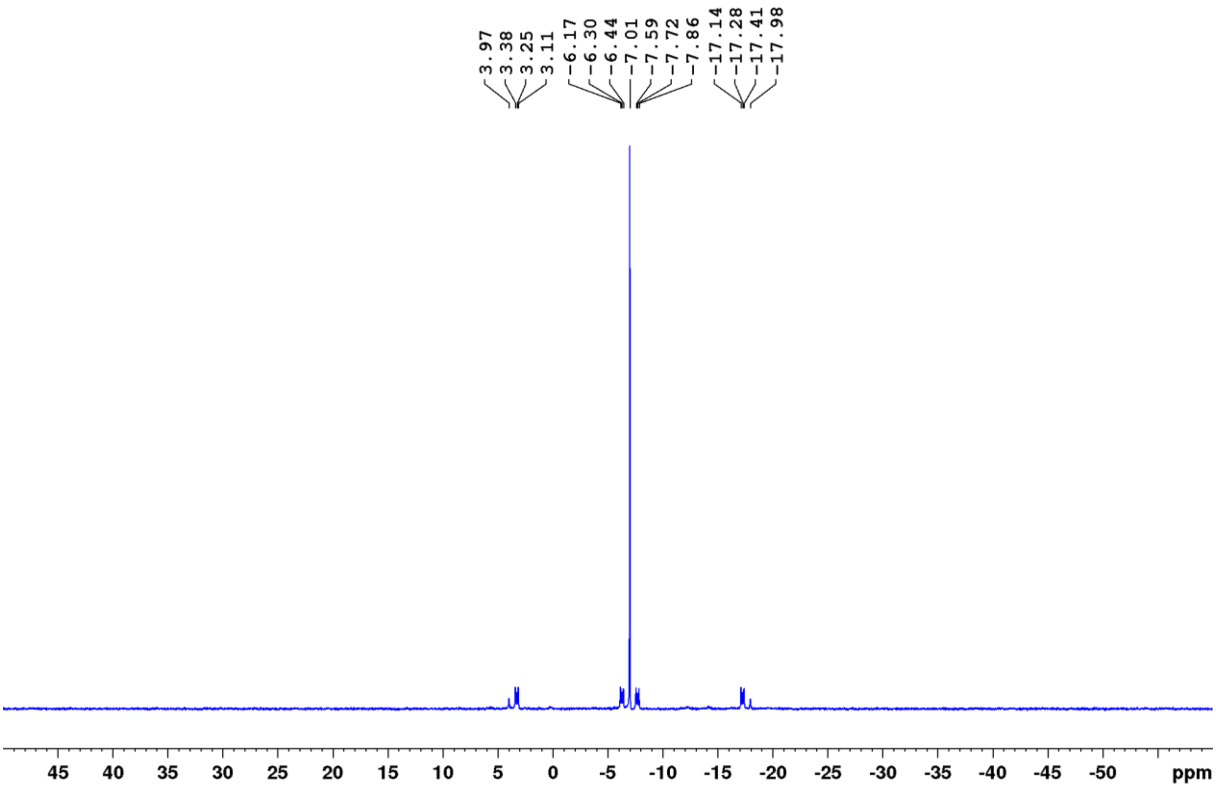

Figure S22. ^{1}H NMR spectrum of **4-Br$^{\mathbf{Cy}}$** in CD_2Cl_2.

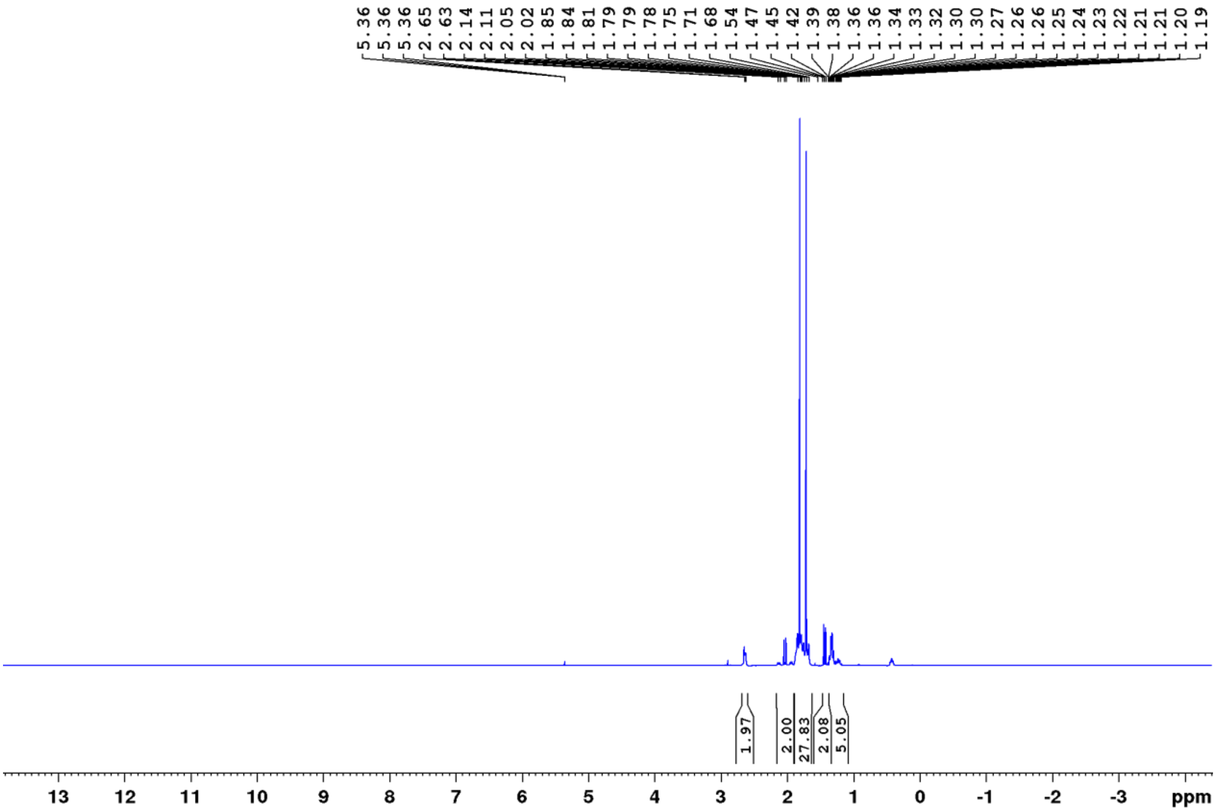

Figure S23. $^{13}C\{^{1}H\}$ NMR spectrum of **4-Br$^{\mathbf{Cy}}$** in CD_2Cl_2.

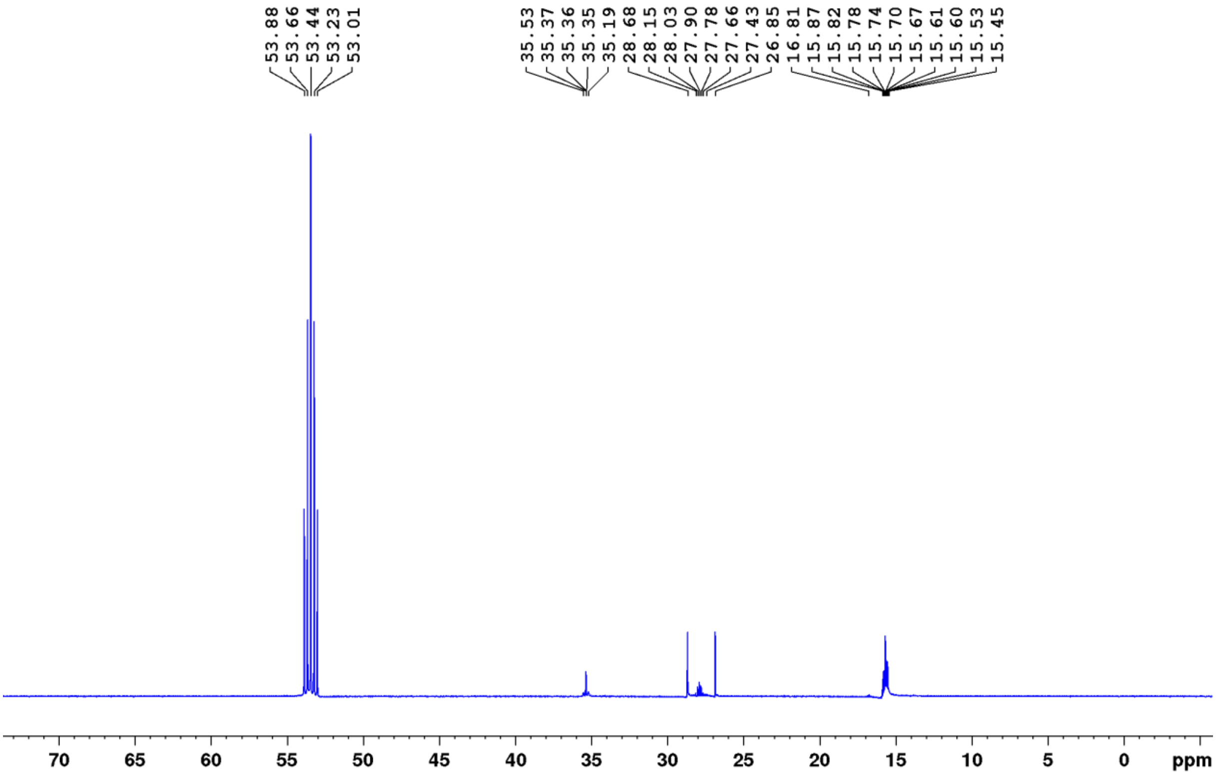

Figure S24. $^{11}B\{^1H\}$ NMR spectrum of **4-Br^{Cy}** in CD_2Cl_2.

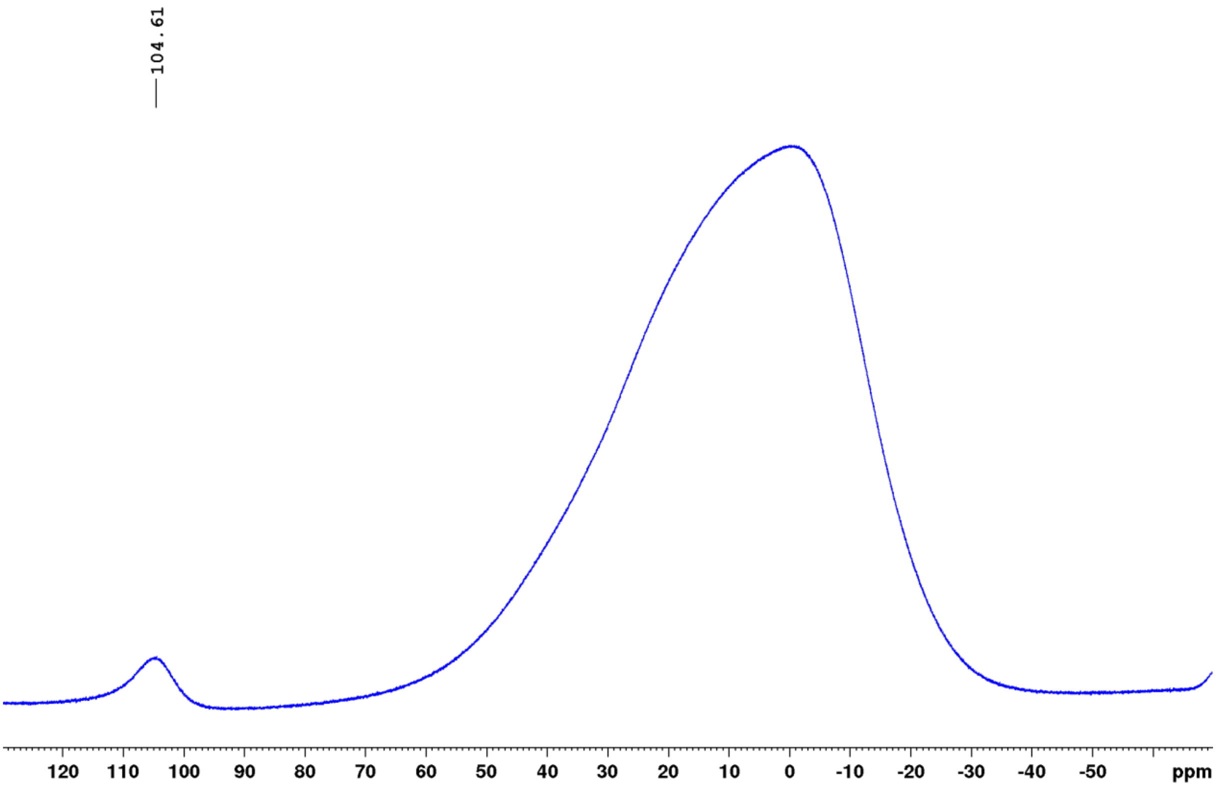

Figure S25. $^{31}P\{^1H\}$ NMR spectrum of **4-Br^{Cy}** in CD_2Cl_2.

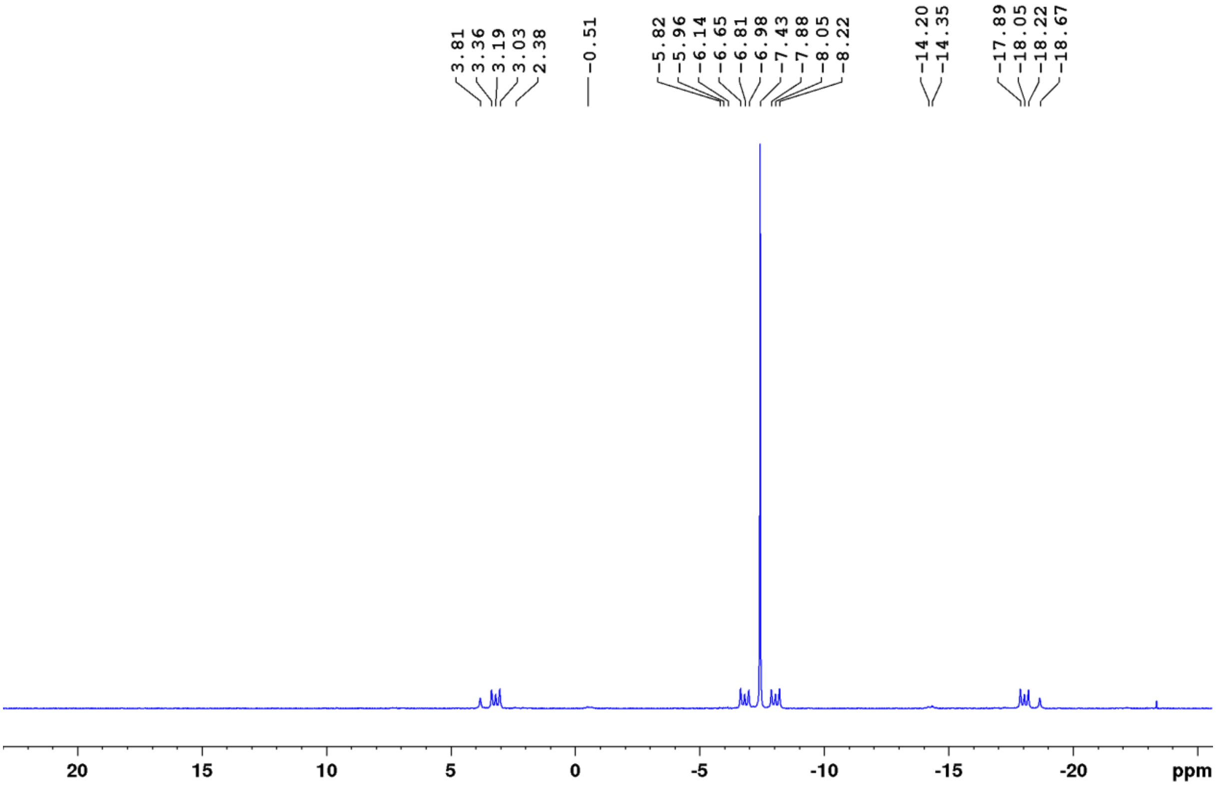

Figure S26. ^{1}H NMR spectrum of **4-Br$^{\mathbf{Mes}}$** in CD_2Cl_2.

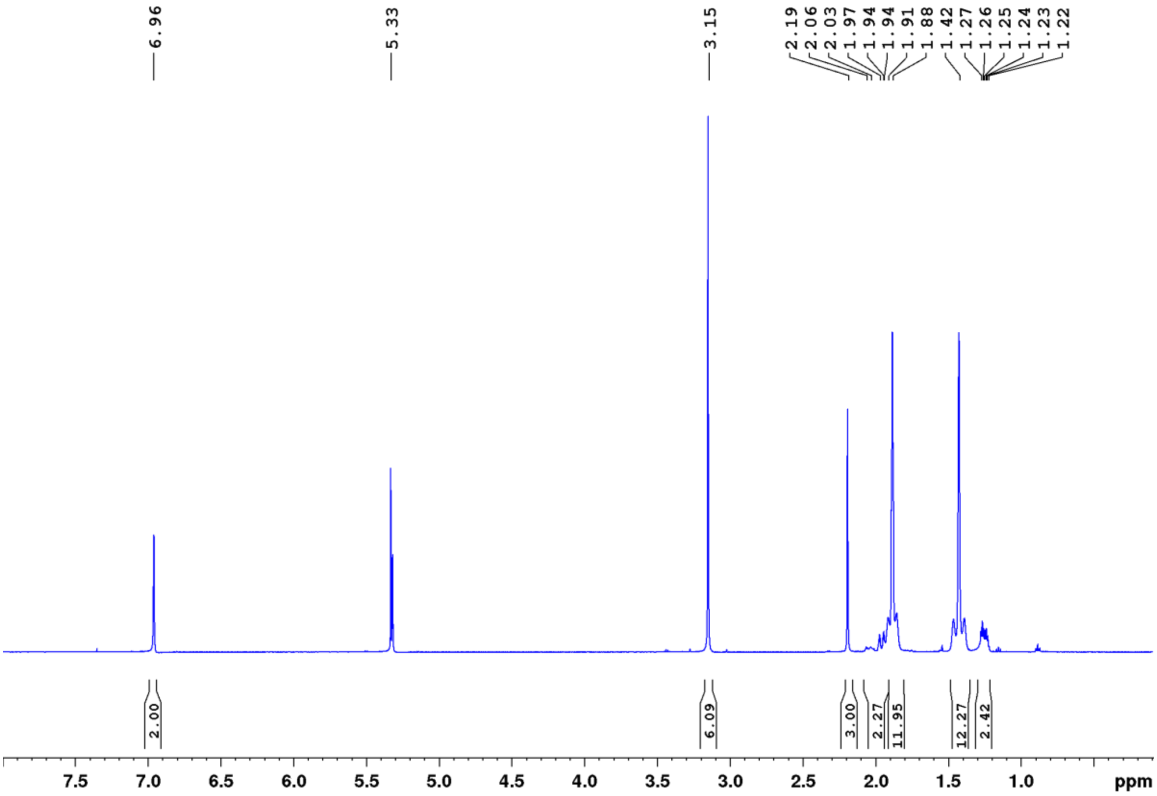

Figure S27. $^{13}C\{^{1}H\}$ NMR spectrum of **4-Br$^{\mathbf{Mes}}$** in CD_2Cl_2.

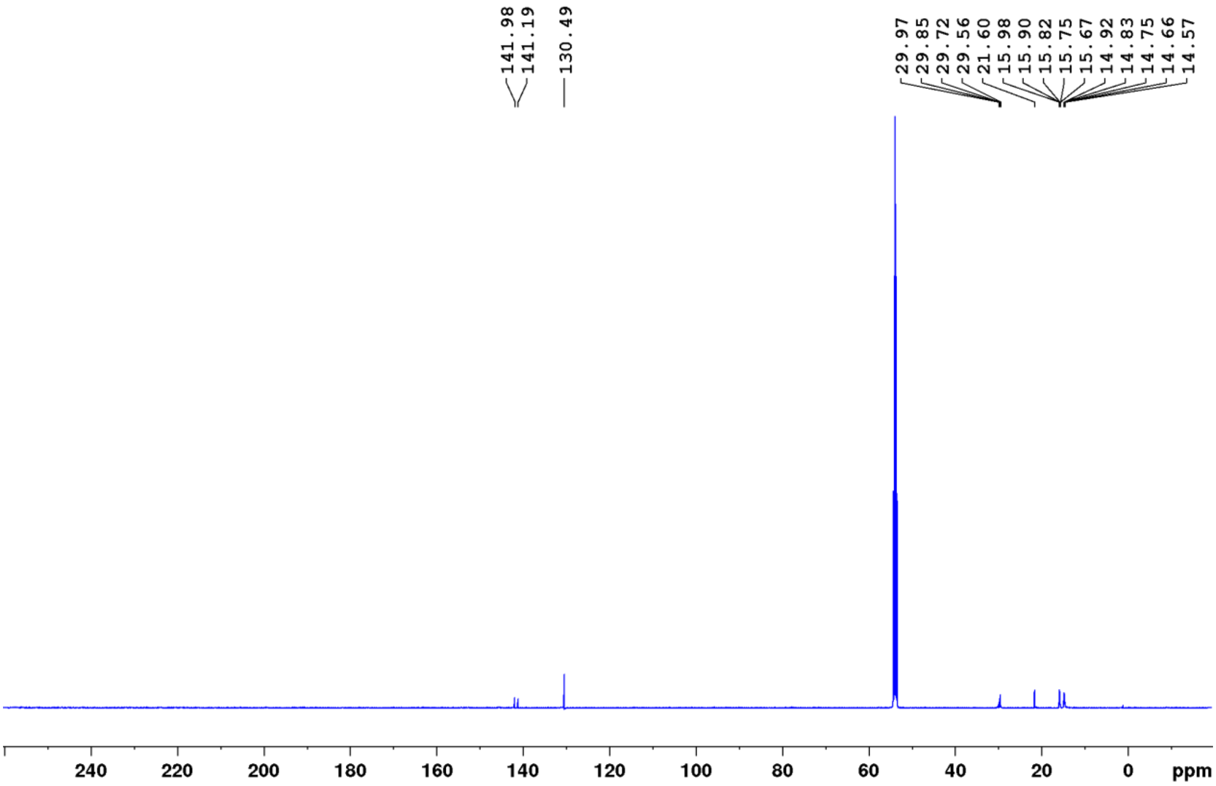

Figure S28. ^{11}B{^{1}H} NMR spectrum of **4-Br$^{\mathbf{Mes}}$** in CD$_2$Cl$_2$.

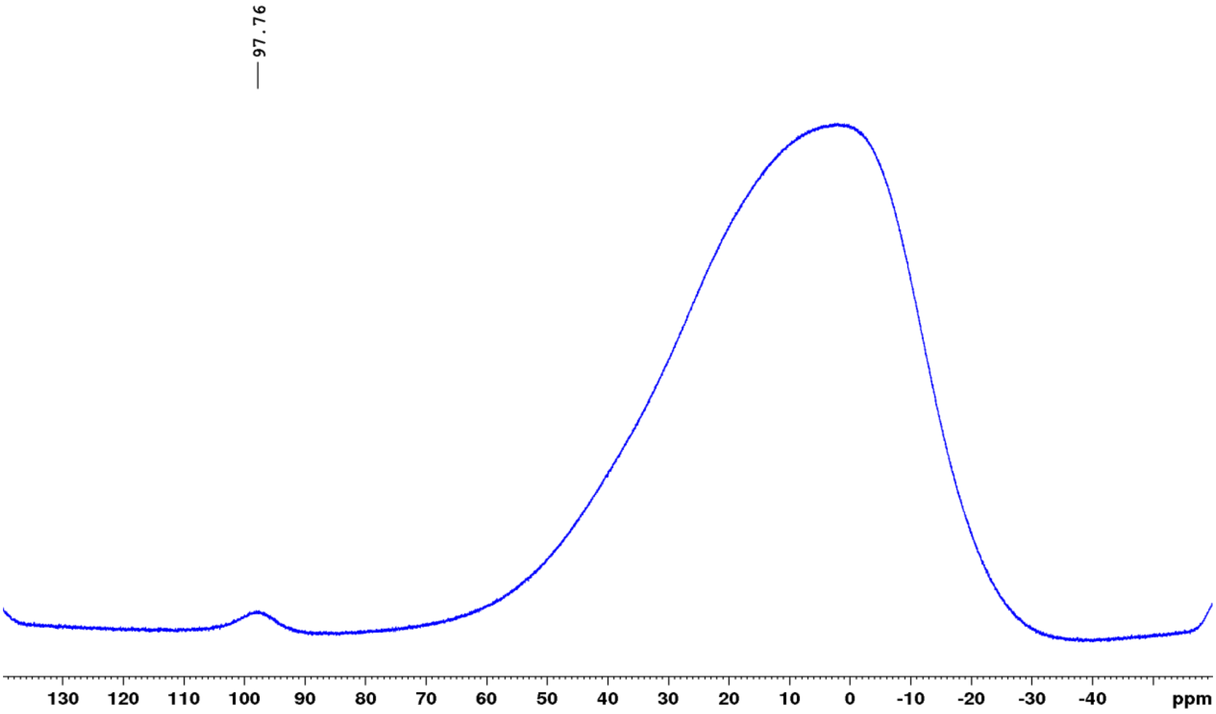

Figure S29. ^{31}P{^{1}H} NMR spectrum of **4-Br$^{\mathbf{Mes}}$** in CD$_2$Cl$_2$.

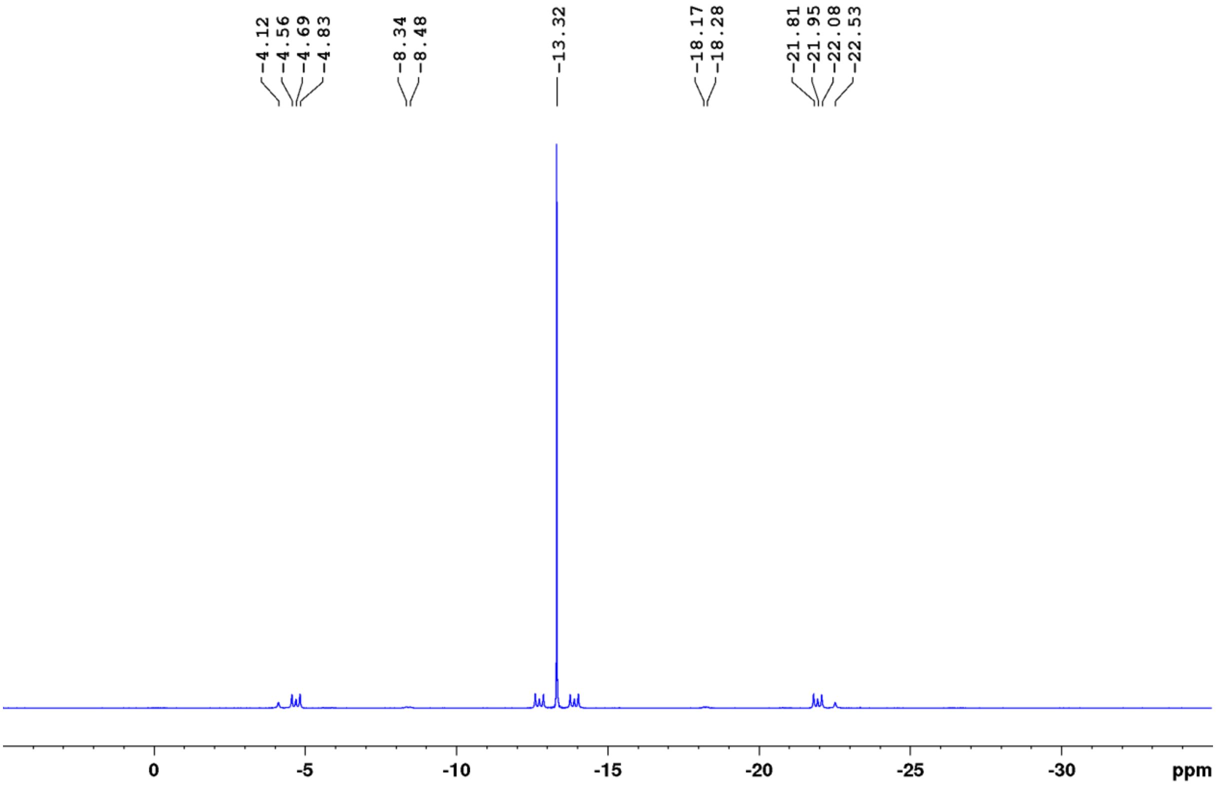

Figure S30. ^{1}H NMR spectrum of **4-I^I** in CD_2Cl_2. The additional resonances at 0.88 ppm and 1.27 ppm correspond to hexane.

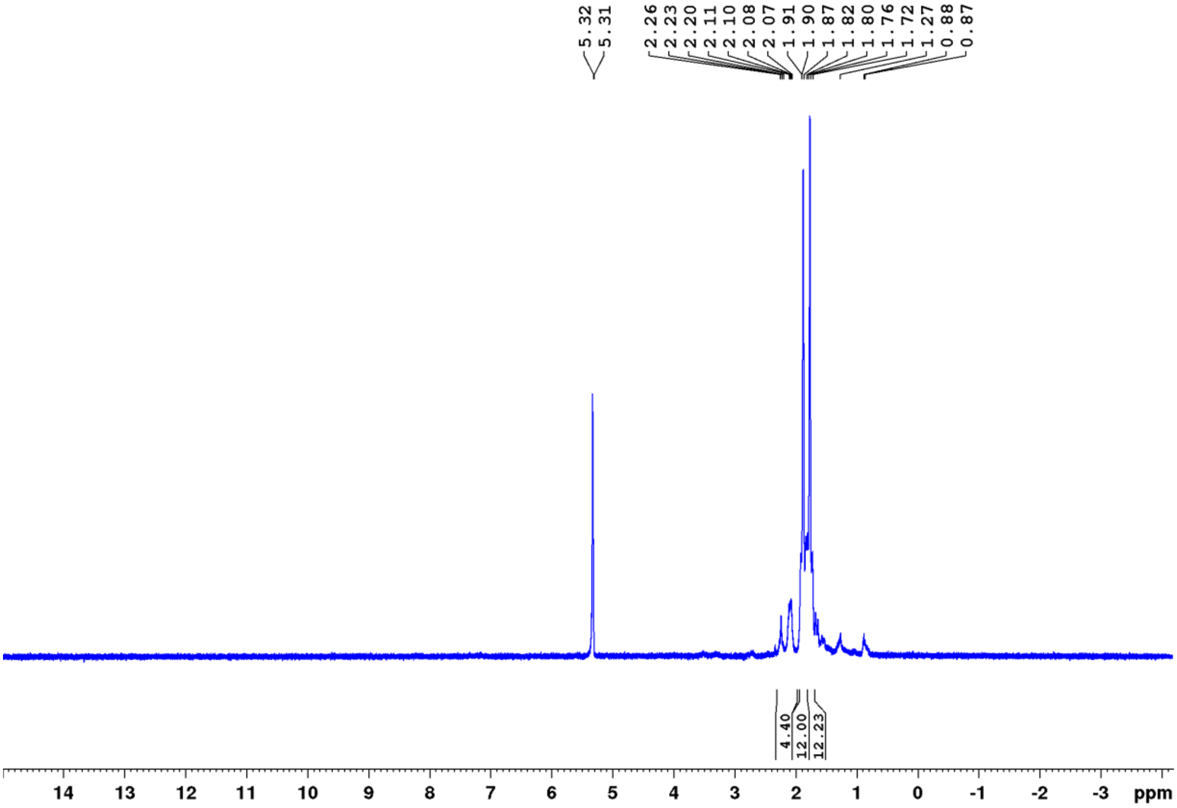

Figure S31. $^{13}C\{^{1}H\}$ NMR spectrum of **4-I^I** in CD_2Cl_2. The additional resonances at 128 ppm correspond to benzene.

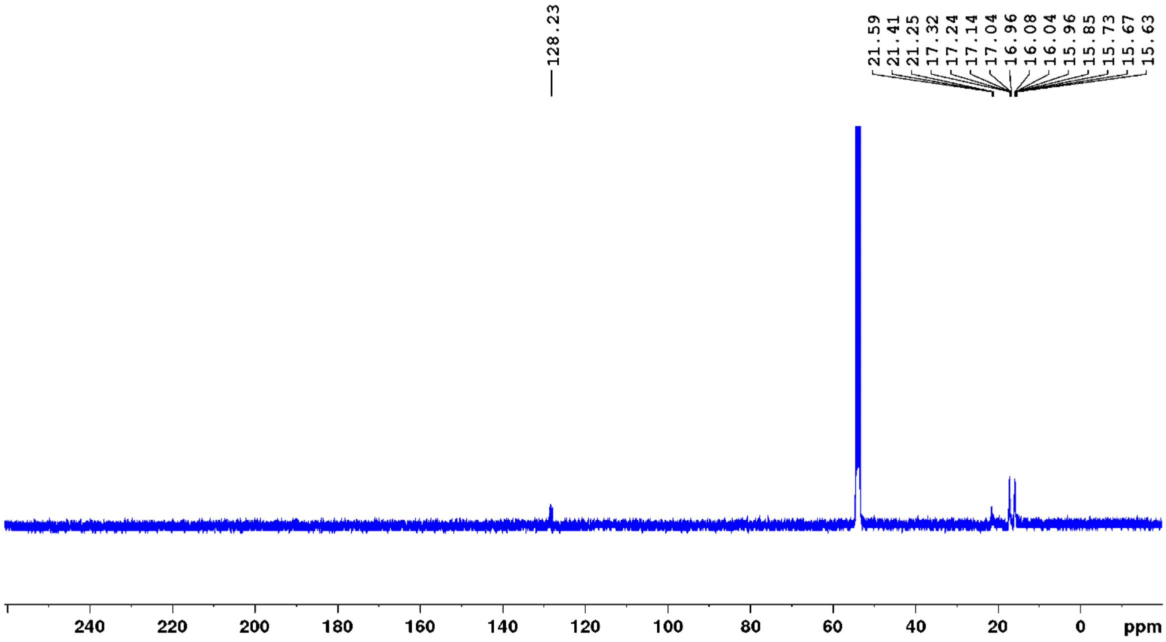

Figure S32. $^{31}P\{^{1}H\}$ NMR spectrum of **4-I^{I}** in CD_2Cl_2. The additional resonance at −35.2 ppm corresponds to the decomposition product **7-I**.

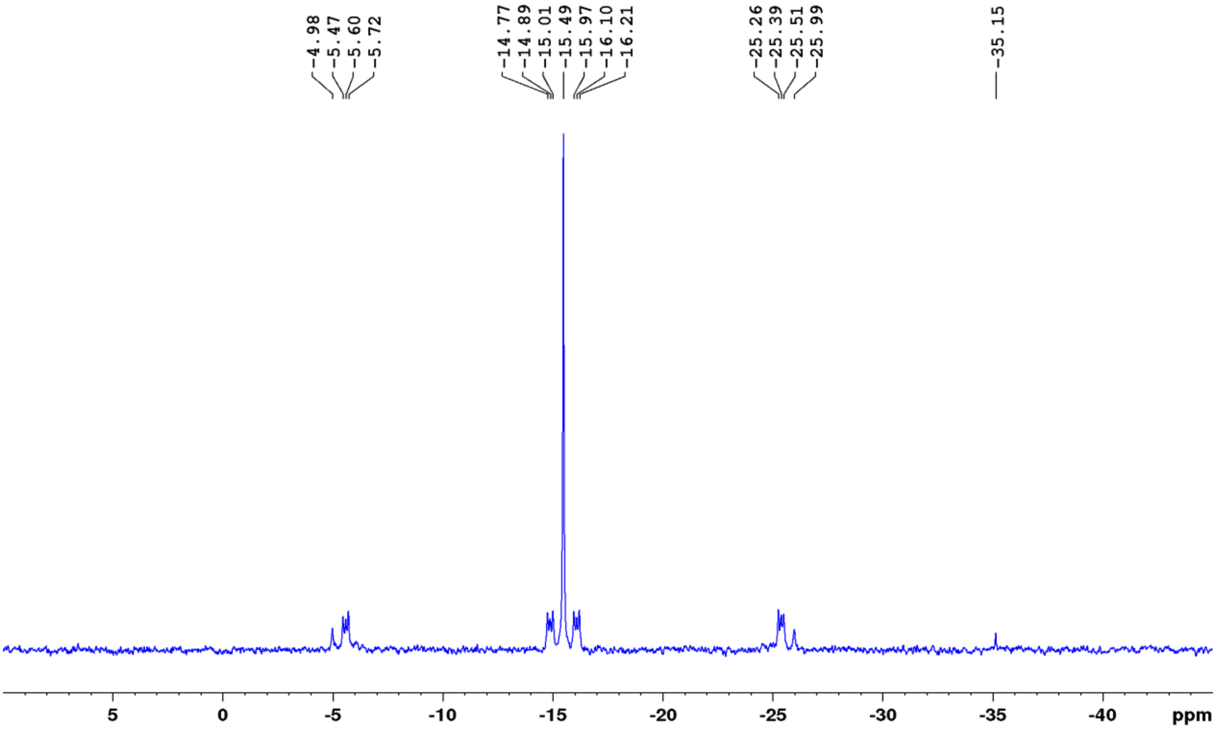

Figure S33. ^{11}B NMR spectrum of **4-I^{I}** in CD_2Cl_2.

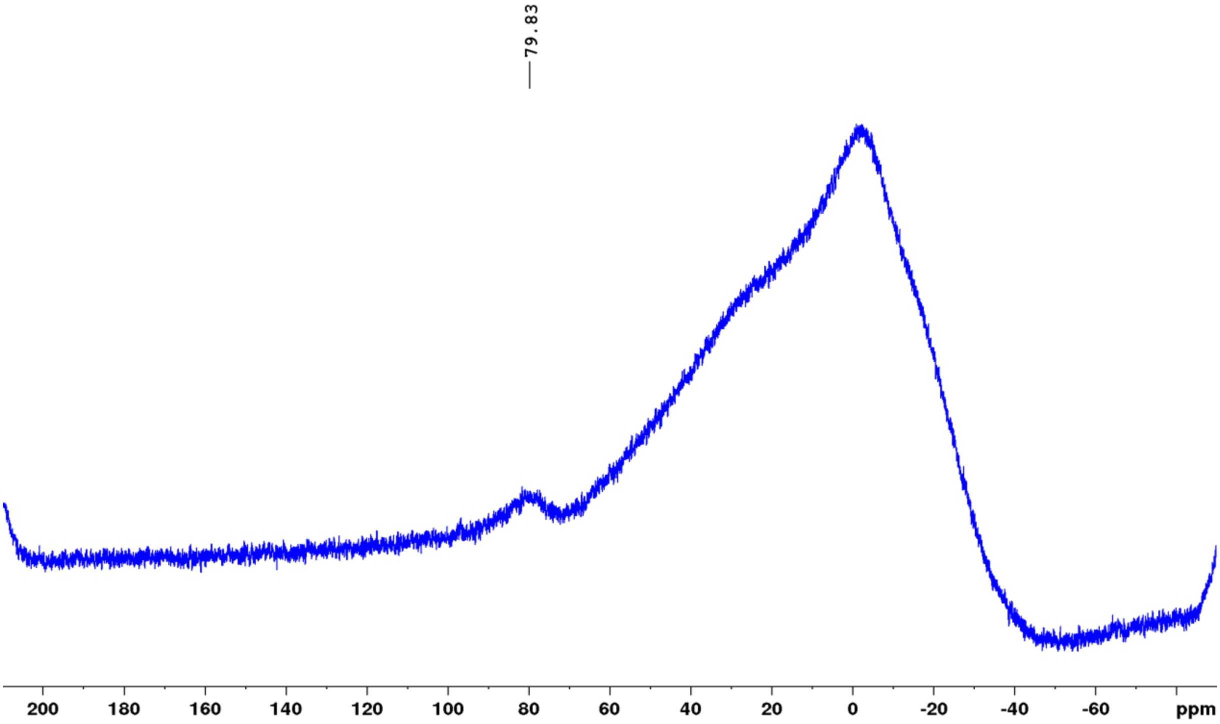

Figure S34. $^{31}P\{^1H\}$ NMR spectrum of **6-I** in CD_2Cl_2.

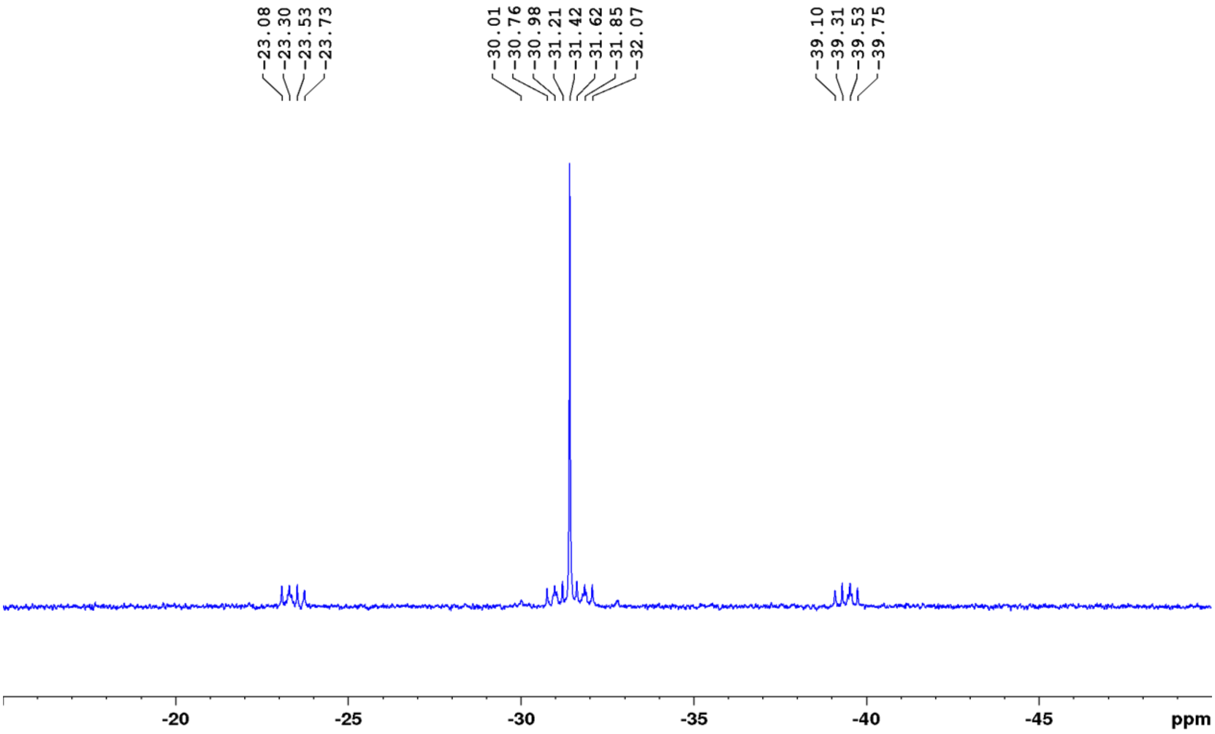

Figure S35. ^1H NMR spectrum of **7-I** in CD_2Cl_2. The additional resonances at 5.33 ppm and 7.35 ppm correspond to dichloromethane and benzene, respectively.

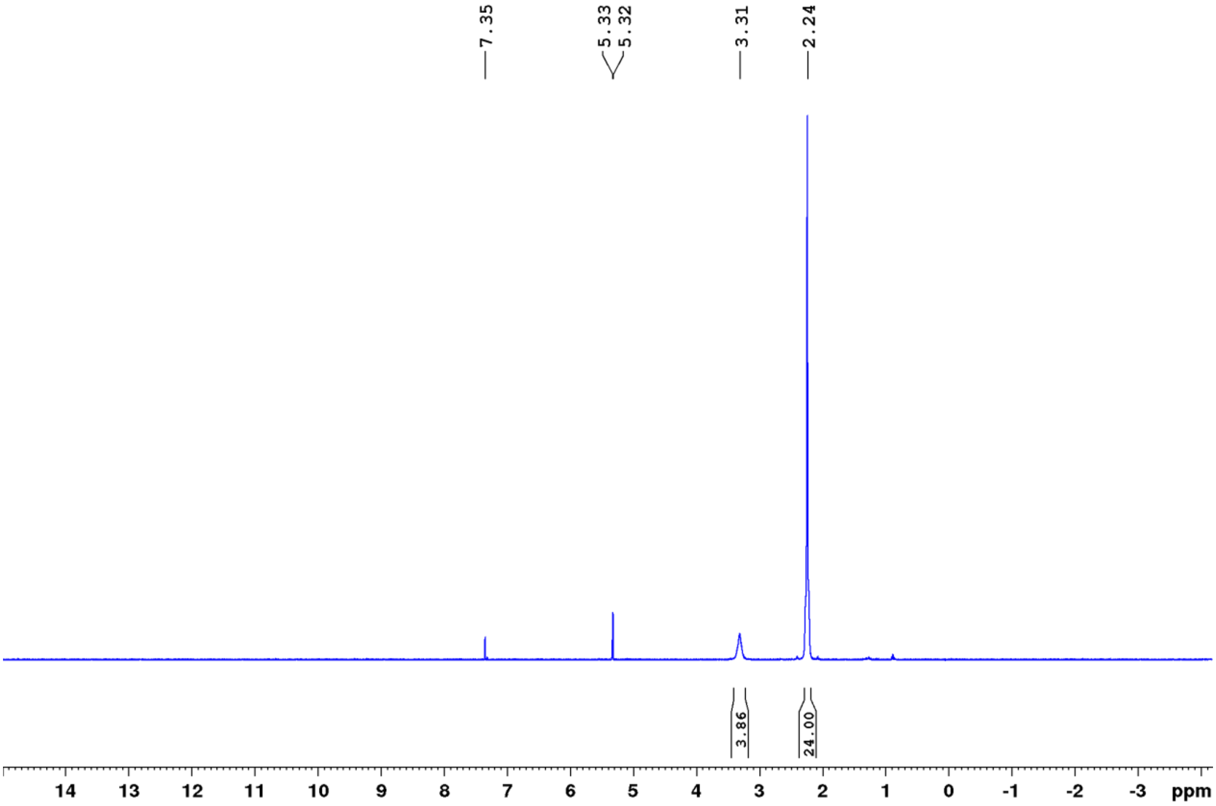

Figure S36. $^{13}C\{^{1}H\}$ NMR spectrum of **7-I** in CD_2Cl_2. The additional resonance at 128.4 ppm corresponds to benzene.

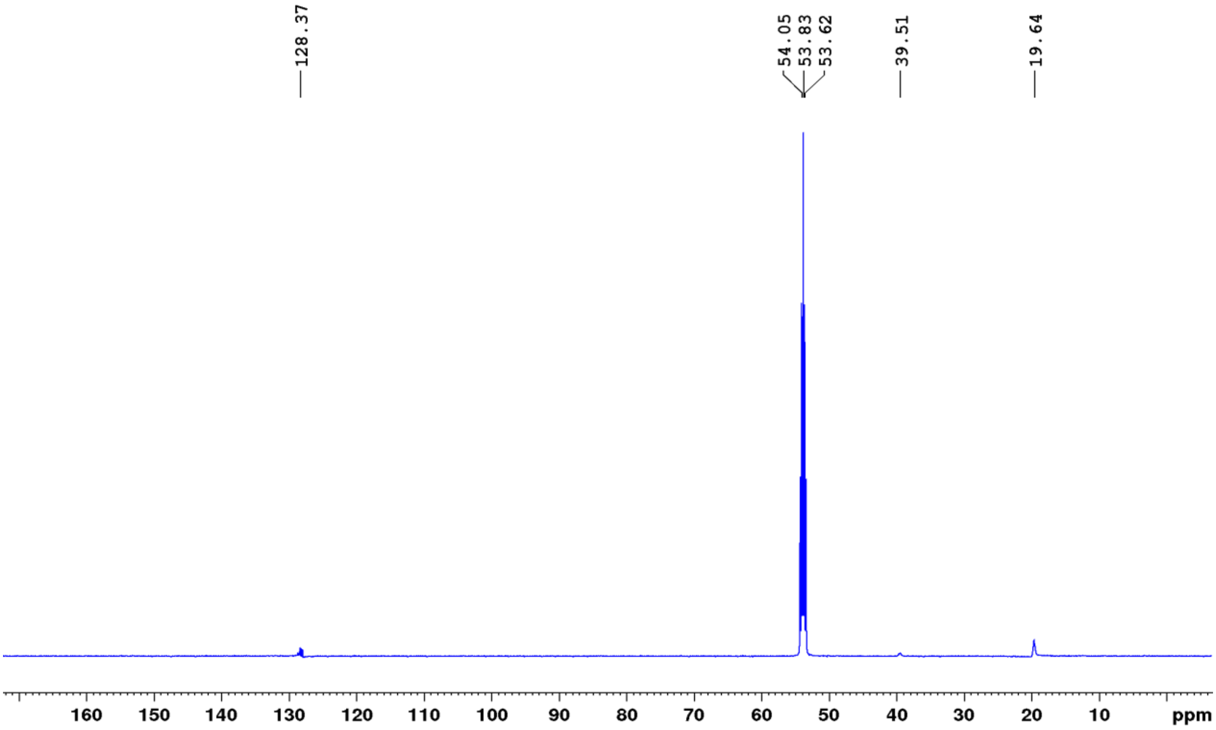

Figure S37. $^{31}P\{^{1}H\}$ NMR spectrum of **7-I** in CD_2Cl_2.

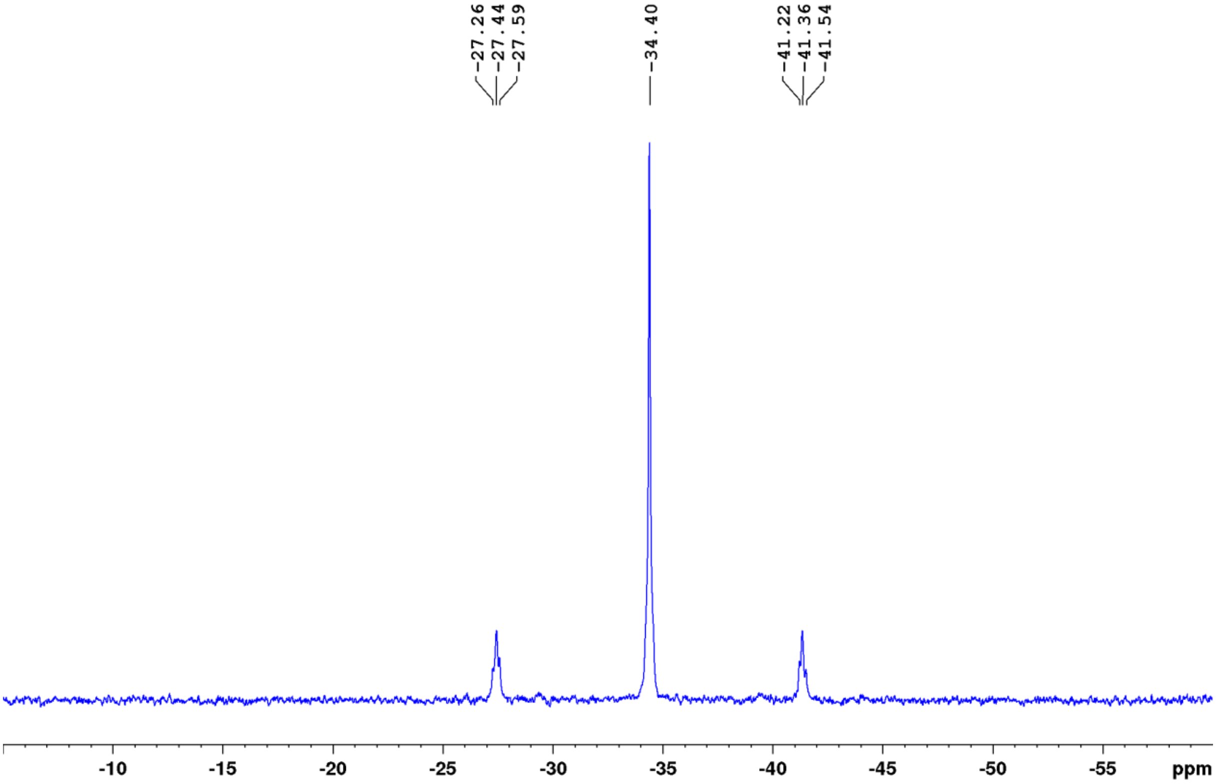

Figure S38. $^{11}B\{^1H\}$ NMR spectrum of **5-Cl^{NMe2}** in CD_2Cl_2.

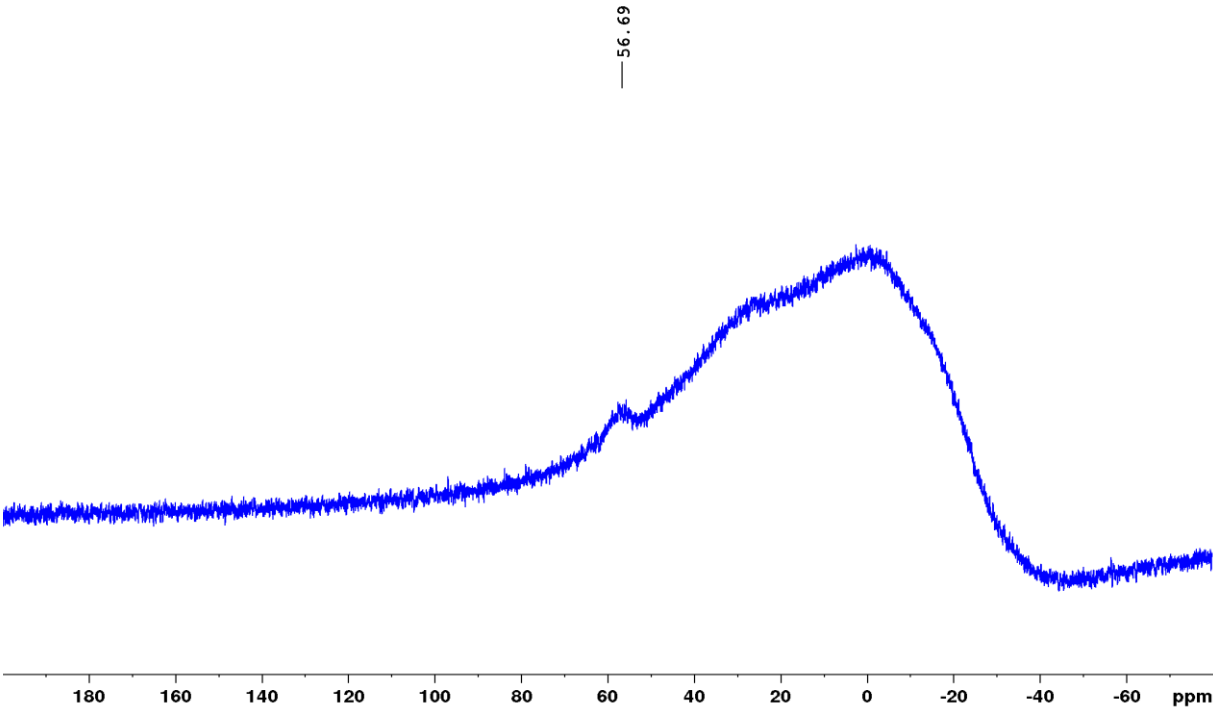

Figure S39. $^{31}P\{^1H\}$ NMR spectrum of **5-Cl^{NMe2}** in CD_2Cl_2.

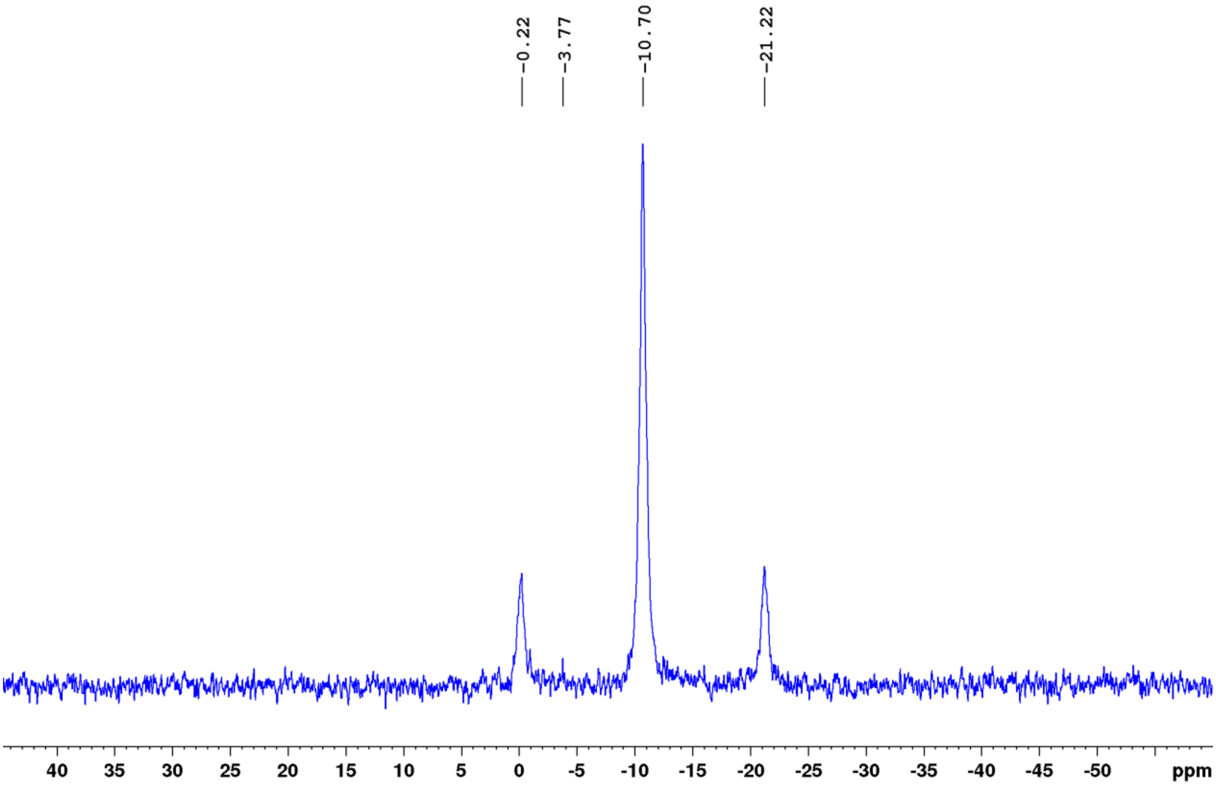

Figure S40. ^{1}H NMR spectrum of **6-Cl** in CD_2Cl_2. The additional multiplets at 0.89 ppm and 1.30 ppm correspond to residual pentane from washing.

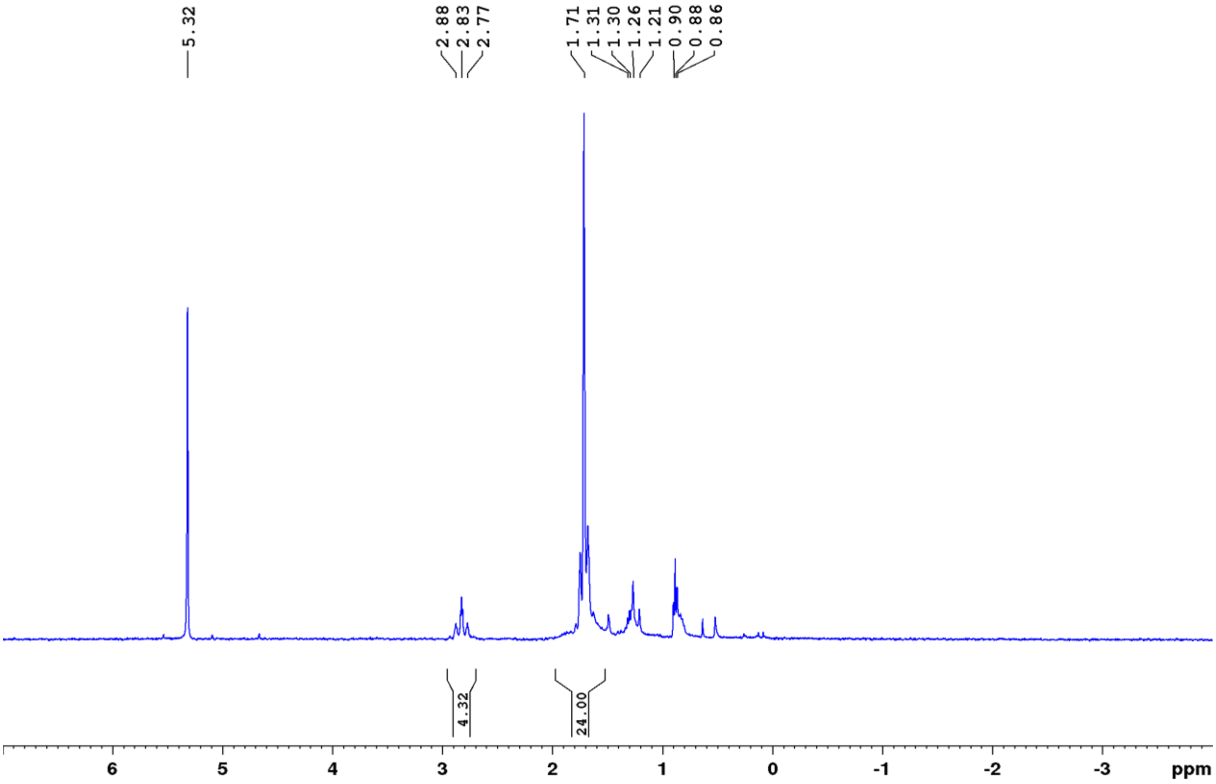

Figure S41. ^{31}P{^{1}H} NMR spectrum of **6-Cl** in CD_2Cl_2.

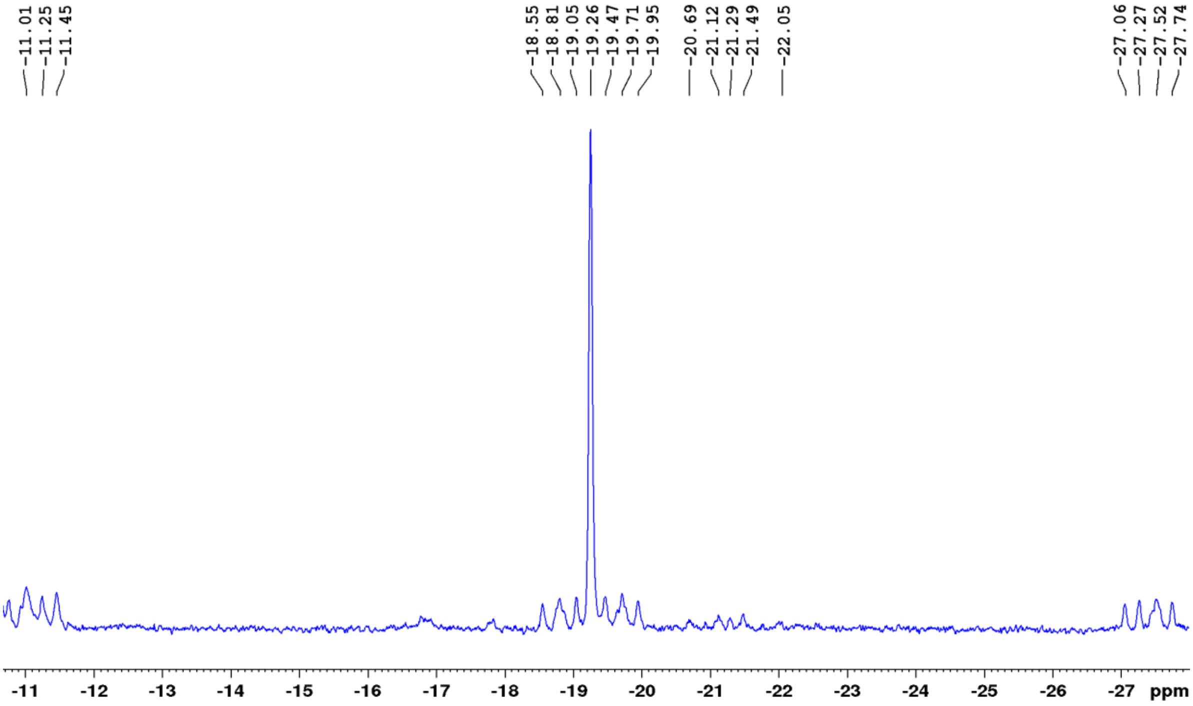

Decomposition of 4-I^{I} and 5-Cl^{NMe2}

Figure S42. $^{31}P\{^{1}H\}$ NMR-spectroscopic monitoring of the decomposition of **4-I^{I}** in CD_2Cl_2 at rt.

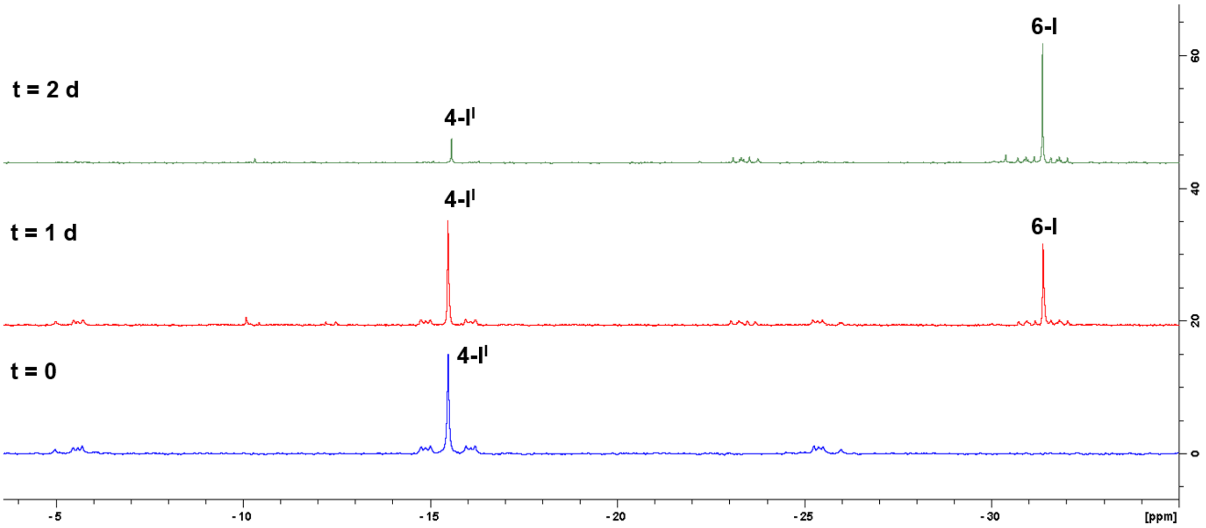

Figure S43. $^{31}P\{^{1}H\}$ NMR-spectroscopic monitoring of the decomposition of **6-I** in CD_2Cl_2.

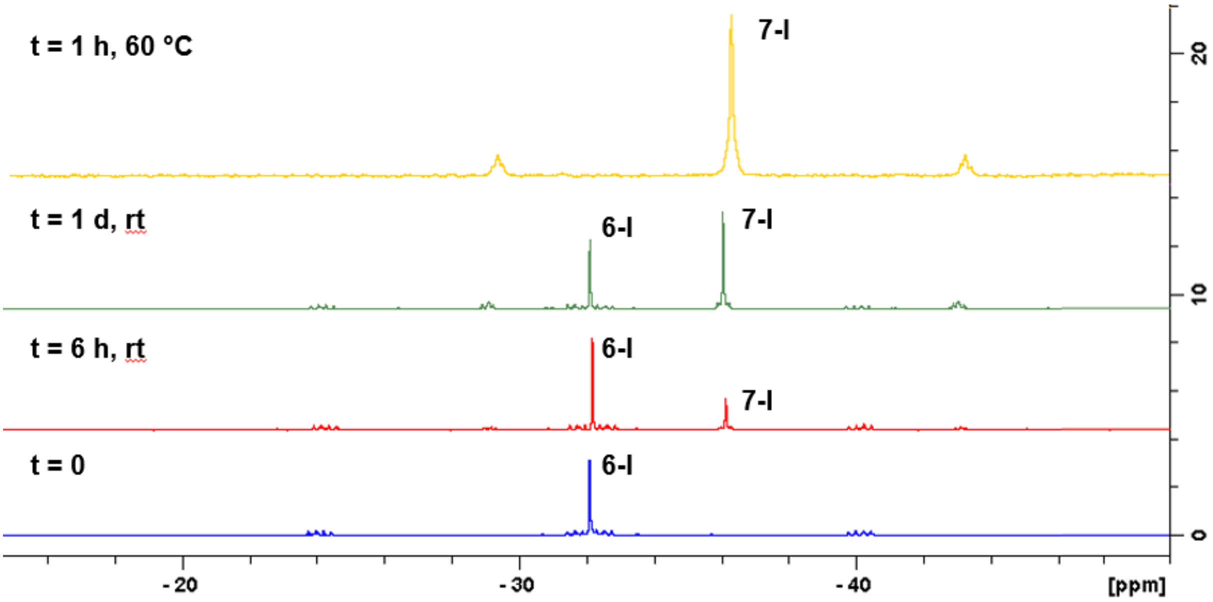

Figure S44. $^{31}P\{^{1}H\}$ NMR-spectroscopic monitoring of the decomposition of **5-Cl^{NMe2}** in CD_2Cl_2 at rt.

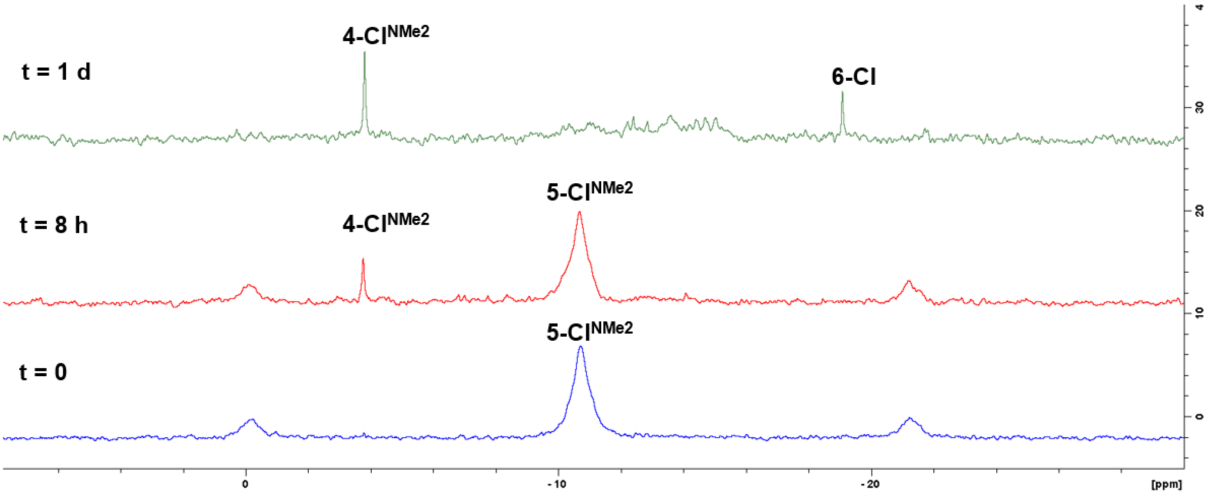

X-ray crystallographic data

Crystal data of compound **4-Br^{Mes}** were collected on a BRUKER X8-APEX II diffractometer equipped with a CCD area detector and multi-layer mirror monochromated Mo$_{K\alpha}$ radiation. All other crystal data were collected on a BRUKER D8 QUEST diffractometer equipped with a CMOS area detector and multi-layer mirror monochromated Mo$_{K\alpha}$ radiation. Structures were solved using the intrinsic phasing method,[10] refined with the SHELXL program[11] and expanded using Fourier techniques. All non-hydrogen atoms were refined anisotropically. Hydrogen atoms were included in structure factor calculations. All hydrogen atoms were assigned to idealised geometric positions.

Crystallographic data have been deposited with the Cambridge Crystallographic Data Center as supplementary publication no. CCDC 2042866 (**1**), 2042867 (**4-Cl^{Tip}**), 2042868 (**5-Cl^{NMe2}**), 2042869 (**6-I**), 2042870 (**7-I**), 2042871 (**4-Cl^{Cl}**), 2042872 (**4-ClN^{Ph2}**), 2042873 (**4-Br^{Mes}**), 2042874 (**3**), 2042875 (**4-Br^{Cy}**), 2042876 (**Pt$_6$ cluster**), 2042877 (**4-I^{I}**), 2042878 (**4-Cl^{Dur}**). These data can be obtained free of charge from The Cambridge Crystallographic Data Centre *via* www.ccdc.cam.ac.uk/data_request/cif.

Refinement details for 1: The displacement parameters of atoms P5 P6 C11 > C15 P2 C4 C5 P3 C6 C7 were restrained to the same value with similarity restraint SIMU 0.002.

Crystal data for 1: $C_{15}H_{42}P_6Pt_2$, M_r = 798.48, red plate, 0.085×0.075×0.021 mm^3, monoclinic space group $P2_1/c$, a = 16.415(5) Å, b = 9.828(3) Å, c = 16.894(8) Å, β = 104.45(2)°, V = 2639.2(17) Å^3, Z = 4, ρ_{calcd} = 2.010 g·cm^{-3}, μ = 10.952 mm^{-1}, F(000) = 1512, T = 100(2) K, R_1 = 0.0495, wR^2 = 0.0681, 6309 independent reflections [$2\theta \leq 55.85°$] and 220 parameters.

Refinement details for 3: The asymmetric unit contains two Pt4 molecules and one hexane molecule disordered over two positions in a 58:42 ratio (RESI HEX). ADPs within RESI HEX were restrained using SIMU and ISOR, 1,2-distances were restrained with DFIX 1.53 0.005 and 1,3-distances with DFIX 2.54 0.005 to fit the known geometry of hexane.

Crystal data for 3: $C_{35}H_{98}P_{14}Pt_4{\cdot}(C_6H_{14})_{0.5}$, $M_r = 1775.10$, yellow block, 0.337×0.258×0.052 mm^3, triclinic space group $P\bar{1}$, $a = 9.7921(6)$ Å, $b = 18.6172(12)$ Å, $c = 35.799(2)$ Å, $\alpha = 86.460(2)°$, $\beta = 82.591(2)°$, $\gamma = 83.964(2)°$, $V = 6428.2(7)$ Å^3, $Z = 4$, $\rho_{calcd} = 1.834$ g·cm^{-3}, $\mu = 9.050$ mm^{-1}, $F(000) = 3420$, $T = 100(2)$ K, $R_1 = 0.0325$, $wR^2 = 0.0491$, 25280 independent reflections [$2\theta \leq 52.044°$] and 1124 parameters.

Refinement details for Pt6 cluster decomposition product of 2: The crystal was heavily twinned but the twinning could not be solved, hence the high residual electron density. The data quality is insufficient for structural discussion but provides proof of connectivity.

Crystal data for Pt6 cluster decomposition product of 2: $(C_{14}H_{40}P_6Pt_3)_2$, $M_r = 1959.11$, colourless needle, 0.242×0.198×0.073 mm^3, triclinic space group $P\bar{1}$, $a = 9.6196(4)$ Å, $b = 11.6672(5)$ Å, $c = 12.3195(5)$ Å, $\alpha = 111.4220(10)°$, $\beta = 93.2400(10)°$, $\gamma = 92.7520(10)°$, $V = 1281.58(9)$ Å^3, $Z = 1$, $\rho_{calcd} = 2.538$ g·cm^{-3}, $\mu = 16.705$ mm^{-1}, $F(000) = 896$, $T = 100(2)$ K, $R_1 = 0.0620$, $wR^2 = 0.1741$, 5619 independent reflections [$2\theta \leq 54.214°$] and 220 parameters.

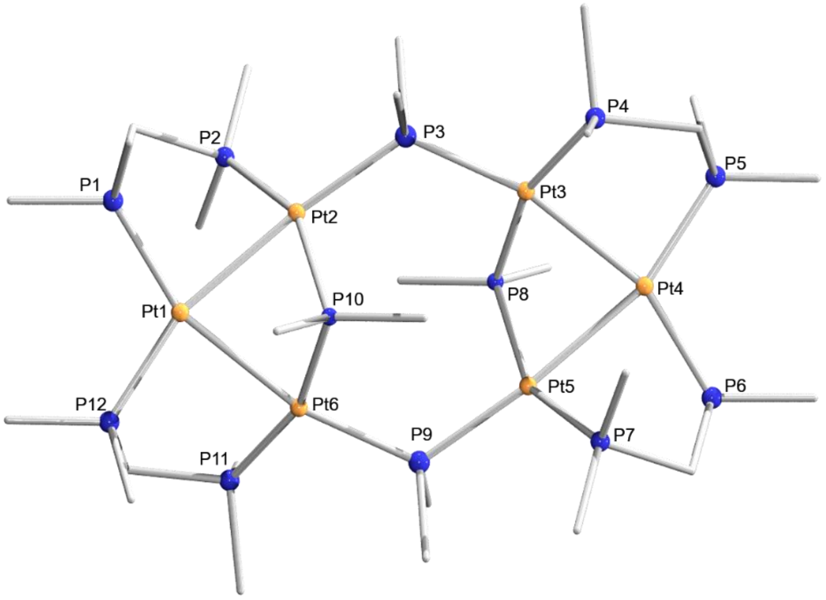

Figure S45. Crystallographically-derived molecular structure of the cluster decomposition product of **2**. Ellipsoids of ligand periphery and hydrogen atoms have been omitted for clarity.

Crystal data for 4-Cl$^{\mathbf{Dur}}$: $C_{20}H_{41}BCl_2P_4Pt_2{\cdot}(C_6H_4F_2)_2$, $M_r = 1105.48$, yellow block, 0.115×0.103×0.099 mm^3, orthorhombic space group $Pbcn$, $a = 11.836(4)$ Å, $b = 22.892(8)$ Å,

c = 14.199(5) Å, V = 3847(2) Å^3, Z = 4, ρ_{calcd} = 1.909 g·cm^{-3}, μ = 7.611 mm^{-1}, F(000) = 2128, T = 100(2) K, R_1 = 0.0240, wR^2 = 0.0404, 4105 independent reflections [2θ≤53.558°] and 211 parameters.

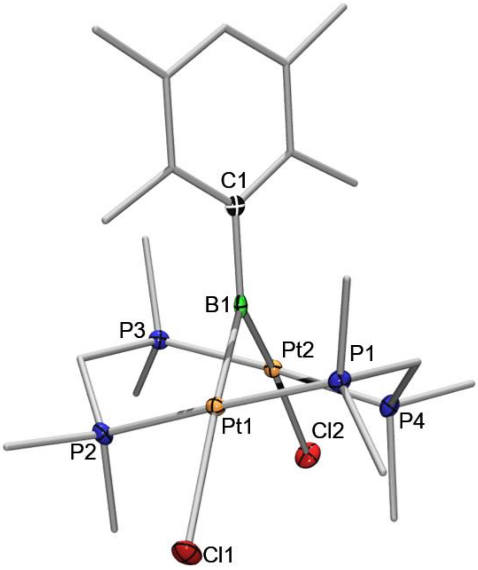

Figure S46. Crystallographically-derived molecular structure of **4-Cl$^{\mathbf{Dur}}$**. Thermal ellipsoids drawn at the 50% probability level. Ellipsoids of ligand periphery and hydrogen atoms have been omitted for clarity.

Refinement details for 4-Cl$^{\mathbf{Tip}}$: The asymmetric unit contains two dichloromethane molecules, one of which is two-fold disordered, modelled in a 34:66 ratio. 1,2- and 1,3-distances within the disorder were restrained using SAME and ADPs using SIMU 0.01

Crystal data for 4-Cl$^{\mathbf{Tip}}$: $C_{27}H_{55}BCl_6P_4Pt_2$, M_r = 1117.28, yellow block, 0.266×0.175×0.119 mm^3, monoclinic space group $P2_1/c$, a = 15.217(7) Å, b = 9.891(3) Å, c = 26.831(9) Å, β = 94.952(14)°, V = 4023(3) Å^3, Z = 4, ρ_{calcd} = 1.845 g·cm^{-3}, μ = 7.522 mm^{-1}, F(000) = 2160, T = 102(2) K, R_1 = 0.0321, wR^2 = 0.0449, 8584 independent reflections [2θ≤53.548°] and 403 parameters.

Refinement details for 4-Cl$^{\mathbf{NPh2}}$: the asymmetric unit contains one solvent molecule, which is half-occupied by a benzene and half-occupied by an *o*-difluorobenzene molecule sharing the same C_6 ring.

Crystal data for 4-Cl^{NPh2}: $C_{25}H_{40}BCl_2NP_4Pt_2{\cdot}(C_6H_4F_2)_{0.5}{\cdot}(C_6H_6)_{0.5}$, $M_r = 969.35$, yellow needle, 0.402×0.117×0.056 mm^3, monoclinic space group $P2_1/c$, $a = 15.0000(5)$ Å, $b = 11.3002(4)$ Å, $c = 19.1129(6)$ Å, $\beta = 93.1650(10)°$, $V = 3234.75(19)$ Å^3, $Z = 4$, $\rho_{calcd} = 1.990$ g·cm^{-3}, $\mu = 9.025$ mm^{-1}, $F(000) = 1844$, $T = 100(2)$ K, $R_1 = 0.0406$, $wR^2 = 0.0615$, 7713 independent reflections [$2\theta \leq 55.776°$] and 344 parameters.

Refinement details for 4-Cl^{Cl}: The structure was refined as a two-component inversion twin using the TWIN keyword. The BASF parameter was refined to 0.46. The asymmetric unit contains two molecules of **4-Cl^{Cl}** and one *o*-difluorobenzene molecule, which was modelled as twofold disordered by rotation around its center in a 57:43 ratio, with the ADP restraint SIMU 0.005. Due to some flexibility in the $Pt_2(dmpm)_2$ framework the ellipsoids of the methyl C1 and C2 groups were highly elongated and restrained to similarity with P1 using SIMU 0.002

Crystal data for 4-Cl^{Cl}: $C_{26}H_{60}B_2Cl_6F_2P_8Pt_4$, $M_r = 1673.18$, colourless block, 0.146×0.141×0.099 mm^3, monoclinic space group $P2_1$, $a = 14.055(2)$ Å, $b = 11.8205(14)$ Å, $c = 15.0133(16)$ Å, $\beta = 98.271(9)°$, $V = 2468.3(6)$ Å^3, $Z = 2$, $\rho_{calcd} = 2.251$ g·cm^{-3}, $\mu = 11.911$ mm^{-1}, $F(000) = 1556$, $T = 100(2)$ K, $R_1 = 0.0145$, $wR^2 = 0.0327$, 10063 independent reflections [$2\theta \leq 52.744°$] and 523 parameters.

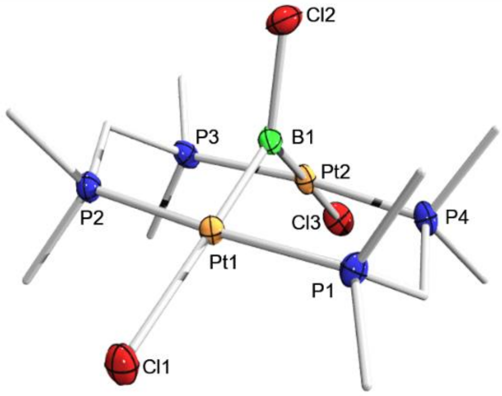

Figure S47. Crystallographically-derived molecular structure of **4-Cl^{Cl}**. Thermal ellipsoids drawn at the 50% probability level. Ellipsoids of ligand periphery and hydrogen atoms have been omitted for clarity.

Crystal data for 4-Br^{Cy}: $C_{16}H_{39}BBr_2P_4Pt_2{\cdot}(CH_2Cl_2)$, $M_r = 1001.09$, colourless plate, 0.805×0.375×0.184 mm^3, monoclinic space group $P2_1/n$, $a = 15.3302(5)$ Å, $b = 10.6045(3)$ Å,

c = 20.0669(6) Å, β = 109.9580(10)°, V = 3066.34(16) Å^3, Z = 4, ρ_{calcd} = 2.169 g·cm^{-3}, μ = 12.109 mm^{-1}, F(000) = 1872, T = 102(2) K, R_1 = 0.0204, wR^2 = 0.0443, 6024 independent reflections [$2\theta \leq 52.044°$] and 261 parameters.

Crystal data for 4-Br$^{\mathbf{Mes}}$: $C_{19}H_{39}BBr_2P_4Pt_2\cdot(CH_2Cl_2)$, M_r = 1037.12, orange block, 0.265×0.197×0.106 mm^3, orthorhombic space group $P2_12_12_1$, a = 10.731(4) Å, b = 15.170(4) Å, c = 19.590(9) Å, V = 3189(2) Å^3, Z = 4, ρ_{calcd} = 2.160 g·cm^{-3}, μ = 11.647 mm^{-1}, F(000) = 1944, T = 100(2) K, R_1 = 0.0120, wR^2 = 0.0258, 6760 independent reflections [$2\theta \leq 53.444°$] and 291 parameters.

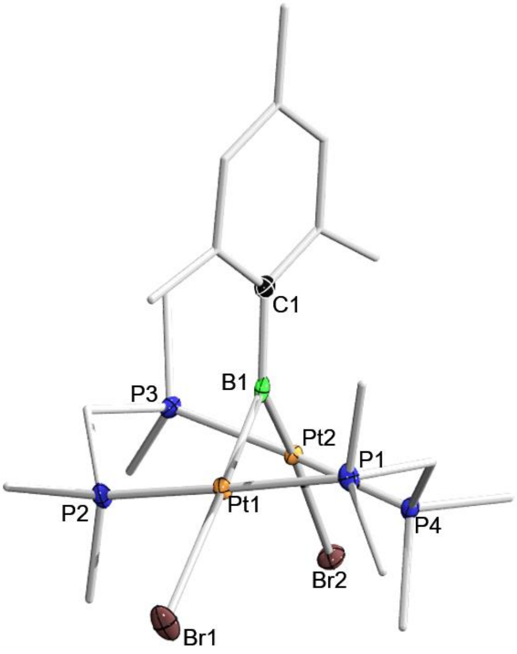

Figure S48. Crystallographically-derived molecular structure of **4-Br$^{\mathbf{Mes}}$**. Thermal ellipsoids drawn at the 50% probability level. Ellipsoids of ligand periphery and hydrogen atoms have been omitted for clarity.

Crystal data for 4-I$^{\mathbf{I}}$: : $C_{12}H_{32}BCl_4I_3P_4Pt_2$, M_r = 1223.74, orange block, 0.364×0.191×0.163 mm^3, monoclinic space group $P2_1/c$, a = 14.9329(9) Å, b = 15.7221(9) Å, c = 26.2447(16) Å, β = 94.570(2)°, V = 6142.1(6) Å^3, Z = 8, ρ_{calcd} = 2.647 g·cm^{-3}, μ = 12.674 mm^{-1}, F(000) = 4416, T = 100(2) K, R_1 = 0.0328, wR^2 = 0.0468, 12566 independent reflections [$2\theta \leq 52.744°$] and 540 parameters.

Crystal data for 6-I: $C_{10}H_{28}I_2P_4Pt_2$, M_r = 916.18, colourless block, 0.434×0.398×0.33 mm^3, monoclinic space group $C2/c$, a = 16.063(5) Å, b = 8.568(2) Å, c = 15.827(3) Å, β = 102.115(14)°, V = 2129.7(9) Å^3, Z = 4, ρ_{calcd} = 2.857 g·cm^{-3}, μ = 16.309 mm^{-1}, F(000) = 1640, T = 100(2) K, R_1 = 0.0398, wR^2 = 0.0901, 2082 independent reflections [$2\theta \leq 52.042°$] and 86 parameters.

Crystal data for 7-I: $C_{16}H_0I_4P_4Pt_2$, M_r = 1213.82, red plate, 0.257×0.154×0.106 mm^3, triclinic space group $P\bar{1}$, a = 8.4725(18) Å, b = 8.5638(18) Å, c = 10.4628(13) Å, α = 111.406(12)°, β = 90.373(7)°, γ = 92.437(8)°, V = 705.9(2) Å^3, Z = 1, ρ_{calcd} = 2.936 g·cm^{-3}, μ = 14.501 mm^{-1}, F(000) = 558, T = 100(2) K, R_1 = 0.0145, wR^2 = 0.0341, 2772 independent reflections [$2\theta \leq 52.032°$] and 122 parameters.

Crystal data for 5-Cl^{NMe2}: M_r = 843.06, orange plate, 0.08×0.06×0.04 mm^3, tetragonal space group $I4_1/a$, a = 17.179(3) Å, b = 17.179 Å, c = 36.881(13) Å, V = 10885(5) Å^3, Z = 16, ρ_{calcd} = 2.058 g·cm^{-3}, μ = 10.706 mm^{-1}, F(000) = 6368, T = 100(2) K, R_1 = 0.0515, wR^2 = 0.0562, 5558 independent reflections [$2\theta \leq 52.744°$] and 247 parameters.

References

1 L. E. Crascall and J. L. Spencer, *Inorg. Synth.*, 1990, **28**, 126.

2 A. Eckert, H. Pritzkow and W. Siebert, *Eur. J. Inorg. Chem.*, 2002, 2064.

3 H. Braunschweig, Q. Ye and K. Radacki, *Chem. Commun.*, 2012, **48**, 2701.

4 H. J. Becher, *Z. anorg. allg. Chem.*, 1957, **289**, 262.

5 R. Soundararajan and D. S. Matteson, *Organometallics*, 1995, **14**, 4157.

6 W. Haubold, J. Herdtle, W. Gollinger and W. Einholz, *J. Org. Chem.*, 1986, **315**, 1.

7 H. Schick, *Dissertation*, Ludwig-Maximilians Universität München, 1966.

8 C. Brunecker, J. H. Müssig, M. Arrowsmith, F. Fantuzzi, A. Stoy, J. Böhnke, A. Hofmann, R. Bertermann, B. Engels and H. Braunschweig, *Chem. Eur. J.*, 2020, **26**, 8518.

9 S. S. M. Ling and R. J. Puddephatt, *Polyhedron*, 1986, **5**, 1423.

10 G. M. Sheldrick, *Acta Cryst.*, 2015, **A71**, 3.

11 G. M. Sheldrick, *Acta Cryst.*, 2008, **A64**, 112.